

N55-32037

(ACCESSION NUMBER)

64

(PAGES)

CR 64440

(NASA CR OR TMX OR AD NUMBER)

(THRU)

1

(CODE)

07

(CATEGORY)

GPO PRICE

\$

CFSTI PRICE(S)

\$

Hard copy (HC)

3.00

Microfiche (MF)

.75

PERIODIC PROGRESS REPORT NO. 3

FOR

STUDY OF COMMUNICATIONS SYSTEMS, AND
DETECTION AND TRACKING SYSTEMS

DESIGN AND FABRICATION OF DYNAMIC CROSSED-FIELD
ELECTRON MULTIPLYING LIGHT DEMODULATOR

20 SEPTEMBER 1964 TO 20 DECEMBER 1964

Contract No.: NAS5-3777

Prepared by

M. Ross
R. Hankin
E. Dallafior
R. Swendsen

The Hallicrafters Co.
5th and Kostner Avenues
Chicago, Illinois 60624

for

Goddard Space Flight Center
Greenbelt, Maryland

ABSTRACT

This third quarterly report presents results of an optical communications and tracking systems program divided into three specific Tasks as follows:

Task I: Analyze laser communications, detection, and tracking systems

Task II: Disseminate the results of Task I through a lecture series, and

Task III: Develop a microwave bandwidth dynamic crossed-field electron multiplier demodulator.

Work in the third quarter is reported for all three tasks.

Task I results for the third quarter include a detailed analysis of optical receiving techniques. Direct photodetection and photomixing are examined. Aspects of photomixing are presented, including spatial requirements of photomixing, local oscillator power requirements, and the present status of photomixing. A comparison of photomixing and direct photodetection is made in which it is shown that the choice of a specific receiving technique must be determined for each particular application. Equations, charts, and graphs are provided.

No lectures were given under Task II in this reporting period.

Task III results for the third quarter consisted of evaluation of factors affecting detector life and in obtaining experimental data on DCFEM operation. A relatively stable detector has been produced that exhibits high current gain and good frequency response. This tube was operated without an auxiliary vacuum pump after being "tipped off" from the pump station. The operating life of this tube was 100 hours. After this time internal gassing decreased cathode response by almost two orders of magnitude.

TABLE OF CONTENTS

<u>SECTION</u>	<u>PAGE</u>
1. TASK I EFFORT	1
1.1 Introduction	1
1.2 Discussion	1
1.2.1 Receiving Techniques	1
1.2.1.1 Direct Photo-Detection	2
1.2.1.2 Photomixing	13
1.2.1.3 Photomixing and Photo-Detection Analysis	16
1.2.1.4 Spatial Requirements of Photomixing	28
1.2.1.5 Local Oscillator Power Requirements	34
1.2.1.6 Present Status of Photomixing	37
1.2.1.7 Some Comparisons Between Photomixing and Direct Photo-Detection	38
1.3 New Technology	41
1.4 Program for Next Reporting Period	42
1.5 Conclusions and Recommendations	42
2. TASK II EFFORT	43
2.1 Introduction	43
2.2 Discussion	43
2.3 New Technology	43
2.4 Program for Next Reporting Period	43
2.5 Conclusions and Recommendations	43
3. TASK III EFFORT	44
3.1 Introduction	44
3.2 Discussion	46
3.2.1 Detector Life	46

TABLE OF CONTENTS (CONT)

<u>SECTION</u>	<u>PAGE</u>
3.2.2 Experimental Results	48
3.3 New Technology	49
3. ⁴ Program for Next Reporting Period	56
3.5 Conclusion and Recommendations	56
BIBLIOGRAPHY	57

LIST OF ILLUSTRATIONS

FIGURE		PAGE
1.	Typical Optical Receiver	3
2.	Pulse Detection System	6
3.	Signal to Noise Ratio as a Function of i_s , T, and B (10 CPS to 1 MC)	8
4.	Signal to Noise Ratio as a Function of i_s , T, and B (1 MC to 10 GC)	9
5.	Normalized Signal Requirements as a Function of Post Detection Power Gain	12
6.	Signal to Noise Ratio when the Non-signal Current to Signal Current Ratio is Greater than Unity for Different i_s/i_{min} Ratios	14
7.	Photomixing Technique	15
8.	Output versus Input Signal to Noise Ratio	18
9.	Optical Balanced Mixer	21
10.	Noise Reduction Due to Balanced Mixer Action for Various Values of K, the Factor of Matching of Detectors, and the Ratio of Reference Noise to Reference Signal r_n/r	23
11.	Noise Suppression with Photomixing	26
12.	Alignment of Signal and Local Oscillator for Photomixing	29
13.	Airy Disk System for Less Critical Angular Alignment for Photomixing	33
14.	Detected Output vs. Angular Mismatch	33
15.	Schematic Diagram of Dynamic Crossed-field Electron Multiplier	45
16.	Cylindrical Cavity Using Non-Contacting Microwave Short Circuit	47
17.	DCFEM (Cylindrical Geometry)	47
18.	Current Gain vs γ	50

LIST OF ILLUSTRATIONS (CONT)

<u>FIGURE</u>		<u>PAGE</u>
19.	Current Gain vs DC Bias	51
20.	Current Gain vs Input Power	52
21.	Optimum Current Gain vs Input Power	53
22.	Optimum γ vs Input Power	54
23.	Optimum DC Bias vs Input Power	55

1. TASK I EFFORT

1.1 Introduction

Task I of the overall program relating to optical communication and tracking systems is a study devoted to theoretical analysis of communications, detection, and tracking systems. Task I will include work as specified below.

A. Emphasize thermal and quantum fluctuations under various conditions and relate microwave noise theory to optical noise theory and the statistical nature of fluctuations.

B. Include an analysis of photomixing and direct photodetection techniques in light of NASA objectives and component state-of-the-art to deduce the minimum noise system for various conditions.

C. Perform a noise analysis of various optical receiving devices in different system configurations in order to establish the minimum noise system for a variety of conditions.

D. Study the effects of the input optical bandwidth and the post detection bandwidth upon system sensitivity.

E. Study the relationship of noise to coherence.

F. Perform a specific noise study concerning the dynamic crossed-field electron multiplier.

Work under Task I in the first quarter included analysis of thermal and quantum fluctuations and the relationship of microwave noise theory to optical noise theory and the statistical nature of radiation. The effects of the input optical bandwidth and the post detection bandwidth on sensitivity were considered. Specific analysis of the system situation for the S-66 was included and preliminary work was presented on applicability of the Goddard Range and Range Rate System to laser systems.

Work in the second quarter was concerned with an analysis of noise sources in laser systems. Noise considerations were related to receiving systems and the Goddard Range and Range Rate System. A comprehensive summary of noise sources was given and aspects of information theory were examined.

Work reported herein under Task I for the third quarter is concerned with optical receiving techniques. Direct photodetection and photomixing are examined in detail and are theoretically analyzed. Aspects of photomixing are presented, including spatial requirements of photomixing, local oscillator power requirements, and the present status of photomixing. Finally, a comparison is made between photomixing and direct photodetection.

1.2 Discussion

1.2.1 Receiving Techniques

A number of receiving techniques can be used for an optical receiver, all of which have direct correlation to microwave receiver techniques.

However, optical receiving techniques are significantly affected by quantum effects, therefore many conceptions of the relative values of amplifiers, detectors, and heterodyne receivers as understood by microwave considerations are no longer valid at optical frequencies. This is particularly true of the "front end" of a laser receiver.

The "front end" of a laser receiver is the most important systems element with regard to sensitivity. There are two basic techniques to choose from, (1) photomixing (a heterodyne technique), and (2) direct photo-detection (a direct detection technique). With either technique a quantum amplifier (optical amplifier) can be used preceding the photomixer or photo-detector to increase gain or selectivity.

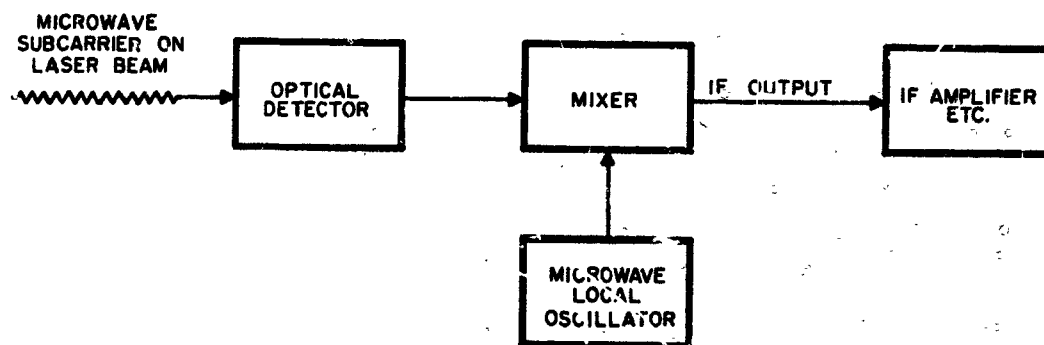
Once past the "front end" there are a number of receiving techniques that can be used. At this point the correlation between RF receivers and optical receivers becomes essentially identical. Hence the following discussion will be primarily confined to the "front end." An example is given in Figure 1, which shows a microwave subcarrier on an optical carrier and a typical use of a microwave mixer and IF amplifier after carrier detection. This particular example is applicable to either front end configuration, i.e., photomixing or direct photo-detection.

1.2.1.1 Direct Photo-Detection

Until recently, direct photo-detection was the only available optical receiving technique. The technique consists of interception and detection of incident energy, or some portion of it, within the confines of the spectral response of the detector. The resultant detected signal is able to follow the amplitude variations induced by the incoming signal modulation. The technique, while similar in conception to an RF crystal detector, is in reality quite different. The optical detector is a photon detector, and thus responds to individual photons at a particular quantum efficiency for every wavelength. It does not respond to total incident energy over a relatively broad RF band where the responsivity is, theoretically, not directly dependent on frequency. In direct photo-detection, all optical frequency and phase information is lost. Similarly, the direct optical detector cannot respond to frequency or phase modulation of the optical carrier. It will reproduce amplitude variations of the incident power when the rate of the variations is less than the frequency response of the detector.

The direct photo-detector can make no distinctions between signal photons and non-signal (background) photons that are within the relatively broad spectral response characteristics. It has no special arrival angle requirement, except that the photon be intercepted by the photo-sensitive area. To achieve background discrimination (if required), one must insert an optical filter; similarly, to achieve spatial filtering, one must reduce the field of view.

The advantage of direct photo-detection is its simplicity. In many cases this results in reduced cost, weight, size and power consumption over other techniques. In general, other techniques would not be used unless the system requirements were such that some technical advantage was attained through their implementation. A common justification for the use of photomixing or the addition of a quantum amplifier is sensitivity, i.e., ability to detect a weaker signal than one can with direct photo-detection. This may take the form of greater



156-003666

Figure 1. Typical Optical Receiver

background rejection or discrimination. To illustrate the technical differences between photomixing and photo-detection capability, the ultimate and the presently attainable sensitivities of direct photo-detection techniques must be established.

An ideal direct photo-detection device can be defined as possessing the capability of detecting each photon within the signal frequency spectrum, detecting no photons outside the signal frequency spectrum, and contributing no internal noise current carriers or photoelectrons. None of these three requirements are satisfied by any presently known photo-detector, i.e., no known photo-detector:

- 1) has a quantum efficiency of unity
- 2) accepts photons over a narrow spectral interval, as would be utilized in a communication or radar system, without responding to photons outside this interval of, at most, 10 gigacycles/sec. (A voice channel can be 3 kc/s wide. Ideally, one would then wish to respond to no more than 6 kc/s optical width).
- 3) has no internal noise

The photo-detectors that come closest to possessing one characteristic usually are worse on the others. However, the second characteristic is unnecessary in the cases where the background is not significant, and can be partially solved with an optical filter in other cases. Filters of 10 Angstroms width are available without special difficulty. This corresponds to about 150 gigacycles/sec. in the visible spectrum.

The sensitivity of the photo-detector can be limited in three ways: (1) by quantum efficiency, (2) by internal noise, and (3) by the background.

In the ideal case the photo-detector would respond such that one photoelectron or equivalent is activated for each photon. Thus, if the incident power is $h\nu n$, $i = qn$. When the quantum efficiency is less than unity, a portion of the signal power is irrevocably lost, so that $i = \epsilon qn$.

When the internal noise of a photo-detector is sufficiently low, such that its sensitivity is dependent only upon the quantum efficiency, then the detector can be considered photon-limited. For this condition the sensitivity of the photo-detector falls short of the theoretically possible sensitivity by the quantum efficiency factor. Thus, if S_T is defined as the theoretical sensitivity, the photon-limited photo-detector sensitivity is given by

$$S = \epsilon S_T \quad (1)$$

The theoretical photon limited sensitivity is given by the fact that in a photo-detector, where there is no phase information, the number of photons are detected as a function of time alone. To detect signals with a

frequency response, B , the maximum response time for detection is given by

$$\tau = \frac{1}{2 \pi B}$$

Another way of looking at this problem is to consider Figure 2, where the time is divided into discrete intervals, t_1, t_2 , etc. The time when a photon arrives can then be assigned to a particular interval, but not to any possible division within the interval. To assign a photon to a particular interval, t_1 , each time interval must be examined separately from the adjacent intervals. Thus, one must be able to say there was a photon received in time t_1 ; there was not any received in time t_2 , etc. To accomplish this, one interval must be discerned from another. Ideally, if the intervals were measured precisely, if the output were positive when there was energy received in a time interval, and if the output were negative when there was no energy received in a time interval, then an output waveform would be obtained as pictured in Figure 2b.

Consider each interval, t , for the decision-making receiver picture in Figure 2a. The incoming pulse and the clock interval feed the "AND" gate such that if both are present the gate operates and a "one" is noted. If there is no incoming received pulse the gate is such that a "zero" is noted. However, instead of a square clock interval, ideally a fundamental wave can be dealt with such that $t = \frac{1}{2B}$. If a perfect gate is assumed, this will function properly.

Since in each interval one photon must be received to denote a "one", it becomes clear that one photon per time-period is required for a time resolution of $t = \frac{1}{2B}$.

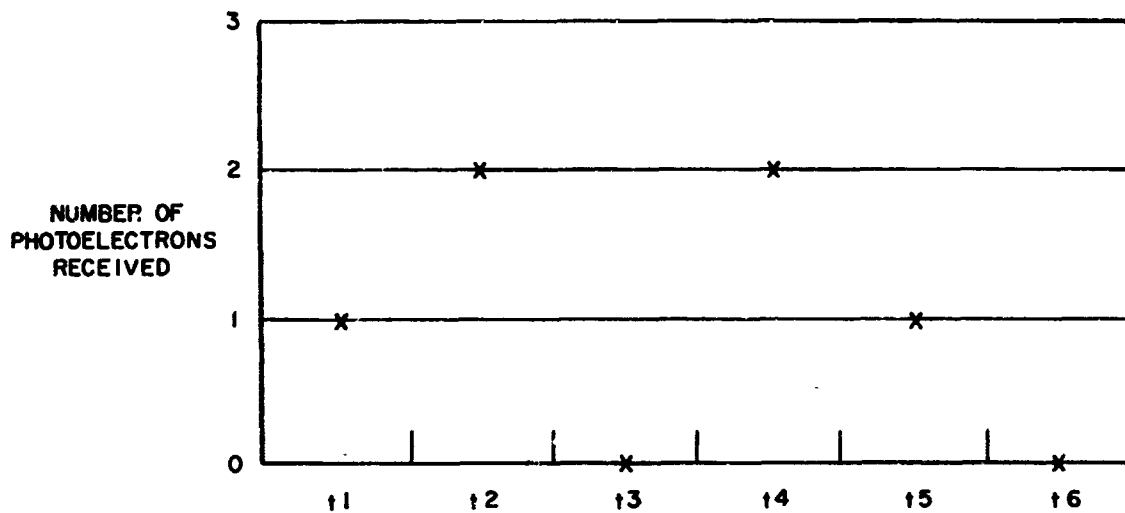
Since $2t$ is the time of one cycle of frequency B , a minimum of two photons per cycle are required in a binary coded system of rate B under the most ideal conditions; that is, the necessary received photons (taking into account the loss due to quantum efficiency) is given by

$$n = \frac{2B}{\epsilon} \text{ in photons/second} \quad (2)$$

In a pulse system of frequency response B , however, it is merely necessary that one effective photon be received in each pulse period, t , where $t = \frac{1}{2B}$; that is, pulse systems with pulse rate, PR , per second requires $\frac{PR}{\epsilon}$

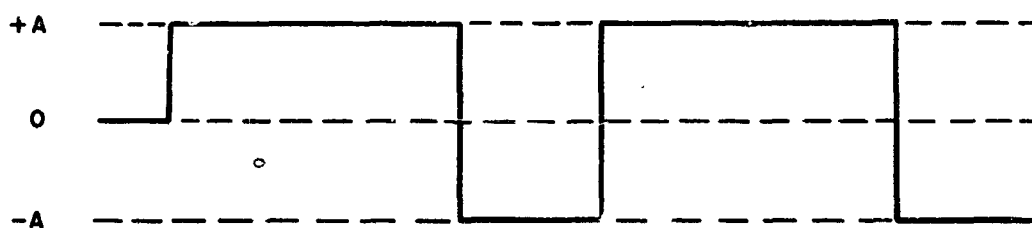
photons per second. The pulse width or time resolution desired will determine the frequency response, B , which has a direct effect on the internal noise.

The internal noise of the photo-detector was discussed in detail in the previous report; however, in this section certain considerations are presented which relate to the conditions under which the photo-detector is internal noise limited. The internal noise consists primarily of shot noise, or its equivalent, and the thermal noise of the output resistance. The internal shot noise, such as in photomultipliers, is given by $i_n^2 R = 2q i_d B R$. It can be seen that frequency response, B , and output resistance, R , enter directly into the amount of internal shot noise to the same extent as the dark current, i_d . However, the frequency response B and output resistance R are not independent. Given the minimum



RECORDED "1" AND "0"

1	1	0	1	1	0
---	---	---	---	---	---



156-005531

Figure 2. Pulse Detection System

output capacity of the detector, C, the output resistance R must not be so large that the time constant, RC will limit the frequency response, B. Since the signal power, given by $i_s^2 R$, is also a direct function of R, the question arises of why R is considered in the ratio of signal power to signal and internal shot noise power given by

$$\frac{S}{N} = \frac{i_s^2}{2qj_d B + 2qi_s B} \quad (3)$$

However, it must be noted that the detector thermal output noise power is given by kTB , and any reduction in R will reduce the output signal power, ¹ but will not affect the thermal noise power in the output resistance, which is independent of the value of R. The total signal to internal and signal noise ratio is then given by

$$\frac{S}{N} = \frac{i_s^2 R}{kTB + 2qi_d B R + 2qi_s B R} \quad (4)$$

The advantage of detectors which inherently possess post-detection gain can be seen from analysis of this equation. If i_s is the output current which has been multiplied by post-detection gain, it improves the S/N ratio over the case of no post-detection gain, and improves it dramatically in the cases where the thermal noise is greater than the internal shot noise.

The internal shot noise is not discriminated against by post-detection gain, since it also is amplified. The thermal noise at the output is not amplified by the detector, however, and in this fact lies the advantage of post-detection gain in the photo-detector.

In many low-level applications the thermal noise will be much greater than the output signal power unless detectors with post-detection gain are employed or a quantum amplifier is employed before the photo-detector. Consider that the resistance, R, is limited by bandwidth, B, and output capacity, C, such that $R \approx \frac{1}{BC}$. Then

$$\frac{S}{N} = \frac{i_s^2}{kTB C + 2qi_d + 2qi_s} \quad (5)$$

Figures 3 and 4 plot equation (5) for different values of B, i_d and T for $C \approx 3$ micro-microfarads.

¹ For the case of narrow-band sub-carrier systems, this is not strictly true since conjugate matching can be accomplished which increases the output power substantially.

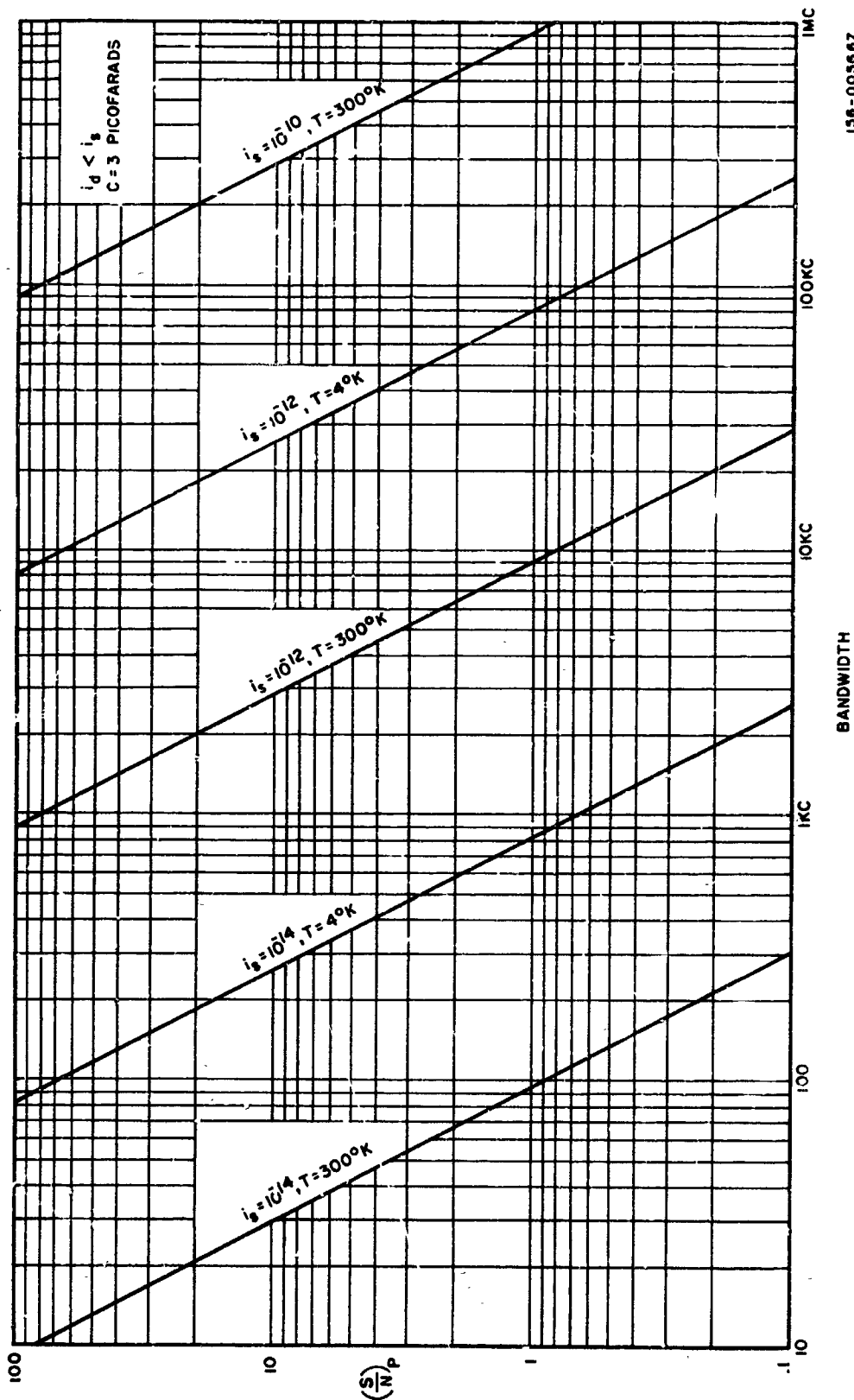


Figure 3. Signal to Noise Ratio as a Function of i_s , T , and B (10 CPS to 1 MC)

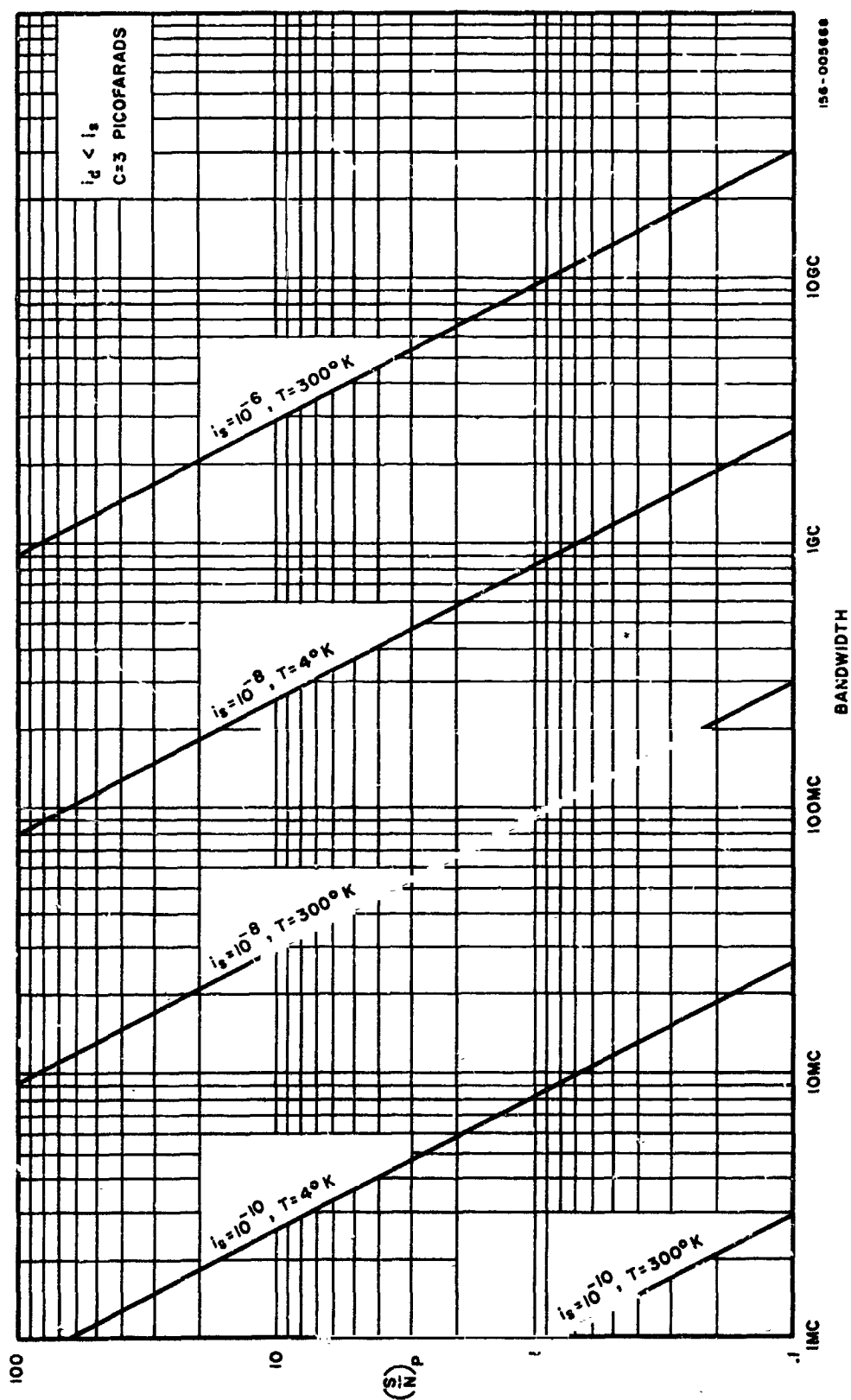


Figure 4. Signal to Noise Ratio as a Function of i_s , T , and B (1 MC to 10 GC)

we find that

$$i_n^2 = 1.2 \times 10^{-32} B^2 + 3.2 \times 10^{-19} i_d B + 3.2 \times 10^{-19} i_s B$$

For typical dark currents that exist, such as in photomultipliers, $i_d < 10^{-14}$ amps, the second terms then become negligible for bandwidths greater than 10 cps, in which case

$$i_n^2 \approx 10^{-32} B^2 + 3.2 \times 10^{-19} i_s B$$

The photon-limited signal is given by

$$i_s = q(2B) \approx 3.2 \times 10^{-19} B$$

The total noise at the photon-limited current is then given by

$$i_n^2 = 10^{-32} B^2 + 6.4 \times 10^{-38} B^2$$

It is clear that the signal-induced shot noise is negligible compared to the thermal noise. Thus, $i_n \approx 10^{-16} B$.

It can now be seen that it will take a signal current approximately three-thousand times the photon-limited condition to attain a SNR of unity. In general, the minimum additional signal current over the photon-limited condition can be determined, for this case of detection without gain, by

$$\frac{(\text{signal current required for SNR} = 1)}{(\text{photon-limited current})} = \frac{\sqrt{KTC}}{2q} \quad (6)$$

Employing a detector with post-detection gain, the detector output signal current is given by

$$i_s^2 = G(i_s')^2 \quad (7)$$

where G is the post-detection power gain and i_s' is the detected photo-current. Relating to equation (5),

$$\frac{S}{N} = \frac{G(i_s')^2}{kTB^2 C + 2qBGi_d + 2qBGi_s'} \quad (8)$$

The signal current requirements for a SNR of unity are reduced substantially by the power gain of the detector. This can be seen clearly if we assume i_s greater than the dark current or background current, and, set equation (8) equal to unity. Thus,

$$Gi_s^2 = KTB^2C + 2qGBi_s$$

When the above is solved for i_s the following is obtained:

$$i_s = qB \left[1 + \sqrt{1 + \frac{KTC}{q^2G}} \right] \quad (9)$$

It is to be noted that when the term KTC/q^2G becomes less than one, the required signal current becomes that of the photon-limited case, $2qB$. In order for the last term to be smaller than one, it is required that

$$G > \frac{KTC}{q} \quad (10)$$

For $T = 300^\circ\text{K}$ and $C = 3$ picroforads, the power gain must be on the order of 10^6 to make the last term negligible. Another gain factor should be added to take into account the thermal noise figure of any amplifier. In general, this factor would be no greater than 10 db, thus raising the total post-detection gain requirements to about 70 db.

Figure 5 plots the results of equation (9) for $C = 3$ picroforads and for different values of T and G . The current requirements are normalized with bandwidth in terms of signal photoelectrons/cps (since $i_s/qB = \bar{n}_s/B$).

It is clear that when post-detection gain is employed much greater sensitivity can be achieved, and that it is possible to find many conditions which are photon-limited. This is the most restrictive case in the sense that nothing more can be done to improve sensitivity.

Insofar as the other shot noise sources are concerned, whenever i_s is greater than both i_d and i_b , the background and dark current noise will be less than the signal shot noise. It is possible for i_d and i_b to be greater than i_s , with the shot noise SNR remaining greater than unity, since

$$\frac{S}{N} = \frac{i_s^2}{2qB(i_s + i_d + i_b)}$$

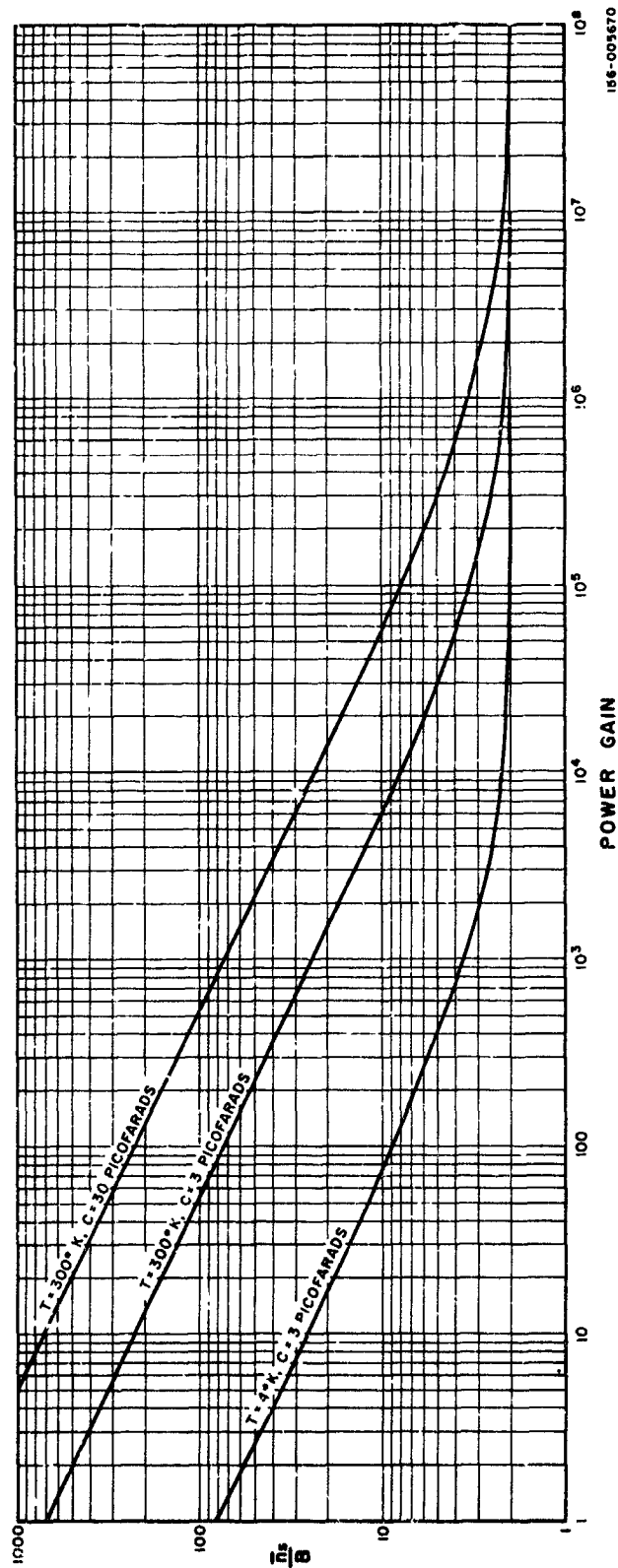


Figure 5. Normalized Signal Requirements as a Function of Post Detection Power Gain.

By considering that the photon-limited current is $i_{smin} = 2qB$, and that the non-signal current is $i = i_d + i_b$, we can re-arrange the above equation into the form,

$$\frac{S}{N} = \frac{i_s}{i_{smin}} \left[\frac{1}{1 + i/i_s} \right]$$

Figure 6 plots this equation for various conditions where the signal to total shot noise ratio is greater than unity although the signal current is less than the non-signal current in the detector. In this normalized form, bandwidth does not appear directly. However, since the photon-limited current is dependent on bandwidth, strong reduction in bandwidth requirements for the same signal current will enable better discrimination against the non-signal currents (i.e., i_s/i_{smin} will increase).

From the presented curves it is clear that at very low signal levels, the signal current cannot be less than the non-signal current without SNR less than unity. At the higher signal levels, the signal currents can be considerably less than the non-signal currents, and still have high SNR.

1.2.1.2 Photomixing

The narrow spectral emission line of the laser has made it possible to obtain mixing action at optical frequencies between two laser sources, one of which can be considered the signal and the other a local oscillator. Thus, it is possible to build an optical heterodyne or homodyne receiver. (Homodyne operation is when the local oscillator is at the same frequency as the optical carrier). Figure 7 illustrates the photomixing technique.

Previous to the development of the laser, complex experiments such as Forresters' indicated the occurrence of photomixing action; however, the lack of a sufficiently narrow spectral source with adequate power made measurements difficult and did not allow practical implementation of photomixing. The first photomixing experiments conducted with the laser were, in fact, measurements of beats between modes of the same laser. (Ref. 1.) These modes were hundreds of megacycles apart and it required a microwave bandwidth phototube, such as the TWP, to detect the beats.

Photomixing, as a receiving technique, was immediately considered. In the first flush of enthusiasm it was assumed the improvement in receiver sensitivity would be similar to that obtained at radio frequencies by use of a superheterodyne receiver rather than a crystal video receiver. While, in general, no such improvement is possible, there remain certain advantages to use of photomixing as a receiving technique compared to direct photo-detection. There are also a number of additional complexities to utilization of a photomixing system.

Photomixing is difficult to understand using the photon concept of light, since each photon is indivisible and is of a particular frequency. Photomixing is best understood by consideration of the wave nature of light (and of all electromagnetic energy). This is consistent with the dual nature of radiation, represented by either waves or particles.

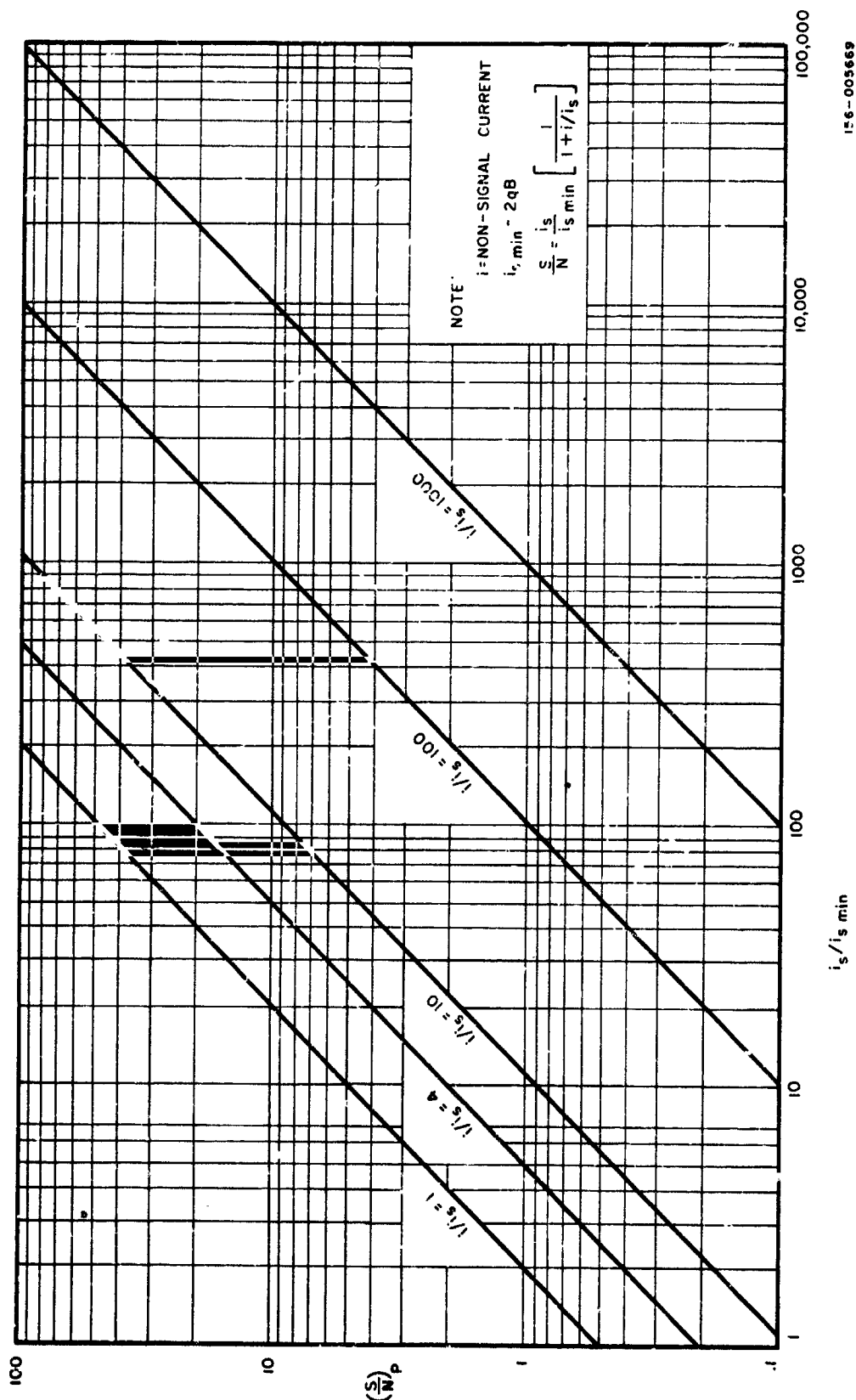
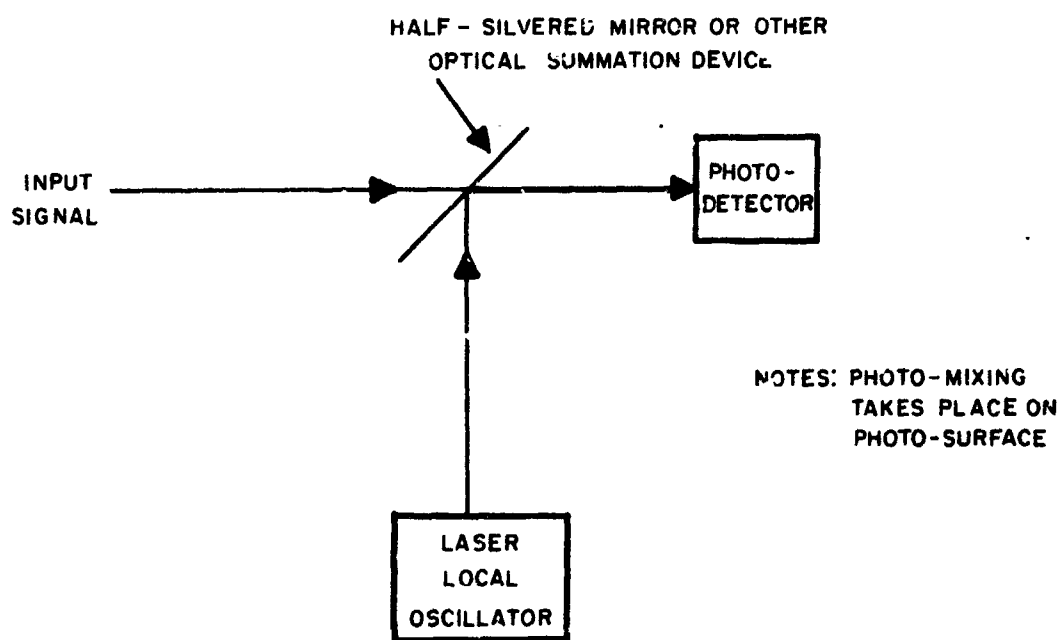


Figure 6. Signal to Noise Ratio when the Non-signal Current to Signal Current Ratio is Greater than Unity for Different $i_s/i_{s \min}$ Ratios



156-005671

Figure 7. Photomixing Technique

1.2.1.3 Photomixing and Photo-Detection Analysis

Photomixing, as in the radio frequency heterodyning processes, is a form of coherent detection, whereas direct photo-detection can be regarded as noncoherent detection. In noncoherent detection, there is no negative output; the detector functions as a rectifying element.

The noncoherent detector response can be expressed as an even infinite series, as follows:

$$e_o = ae_i^2 + be_i^4 + ce_i^6 + \dots \quad (11)$$

Generally, one can ignore the higher order terms. A good approximation is that $e_o = ae_i^2$, i.e., the rectifier is a square-law detector. A photo-detector is an ideal square-law device in which the higher terms of (11) are not present.

In square-law detection, the output signal-plus-noise ($s_o + n_o$) is related as follows to the input signal-plus-noise ($s_i + n_i$):

$$s_o + n_o = a(s_i + n_i)^2 = a(s_i^2 + 2s_in_i + n_i^2) \quad (12)$$

a is usually a constant and the output signal to noise ratio is given by

$$s_i^2 / (2s_in_i + n_i^2) \quad (13)$$

It is seen the noise consists of two terms: one (n_i^2) due to beats between the noise components, and the other ($2s_in_i$) due to beats between the signal and noise. If the input signal-to-noise ratio is much less than unity ($n_i \gg s_i$), n_i^2 is much greater than $2s_in_i$. Thus, the output noise and signal are approximately

$$s_o \approx as_i^2 \quad (14)$$

$$n_o \approx an_i^2 \quad (15)$$

The output signal-to-noise ratio for this condition is given by

$$\frac{s_o}{n_o} \approx \left(\frac{s_i}{n_i} \right)^2 \quad (16)$$

It is clear from the above equation that the SNR is degraded considerably for an input SNR less than one. Figure 8 illustrates the relation of equation (16). However, at optical frequencies, where the noise-in-signal is of importance, the input SNR can never be less than one when the fluctuation noise of the signal is considered. The fluctuation noise of the signal must necessarily be less than the signal itself, and as discussed in earlier sections, can be considered proportional to the square root of the signal photons, n_s . Also, the internal detector noise is not considered as part of the input noise power to the detector. Thus, in essence for noncoherent detection, it is only the background energy that would reduce the input SNR to less than unity and thus cause degradation of the SNR. It is to be noted that if n_b is the number of received background photons in some reference time, t , the effective input SNR for $n_b \gg n_s$ is given by

$$\frac{s_i}{n_i} \approx \frac{\sqrt{\epsilon} n_s}{1/2} \quad (17)$$

n_b

Now consider coherent detection using the same detection device. The important difference is that prior to the detector a local oscillator signal is added to the input signal. The local oscillator can be considered a coherent reference whose amplitude is much larger than the input signal or noise. Designating this reference as r , the total voltage into the detector is given by

$$e_i = (s_i + n_i + r) \quad (18)$$

For the same square-law detector as before, the output voltage is

$$e_o = ae_i^2 = 2ar(s_i + n_i) + a(s_i + n_i)^2 + ar^2 \quad (19)$$

if $r \gg (s_i + n_i)$, the second term is negligible in comparison to the first, and can be ignored. If the reference is a pure sinusoid, the quantity ar^2 is a constant and can be regarded as a direct current and theoretically will be unimportant. The output voltage can be expressed, based on the foregoing simplifications, as

$$e_o = 2ar(s_i + n_i) \quad (20)$$

Interpretation of the above equation is that the reference beats with the signal and noise and converts the signal spectrum down to a lower frequency, which is the difference between the reference oscillator and the signal frequency; that is $f_{IF} = |f_s - f_r|$, where the difference frequency is usually the center frequency of an IF amplifier. The coherence is not achieved by the detector itself, but rather by the addition of the reference with the signal prior to the detector. Because of this addition, correlation is actually performed within the detector.

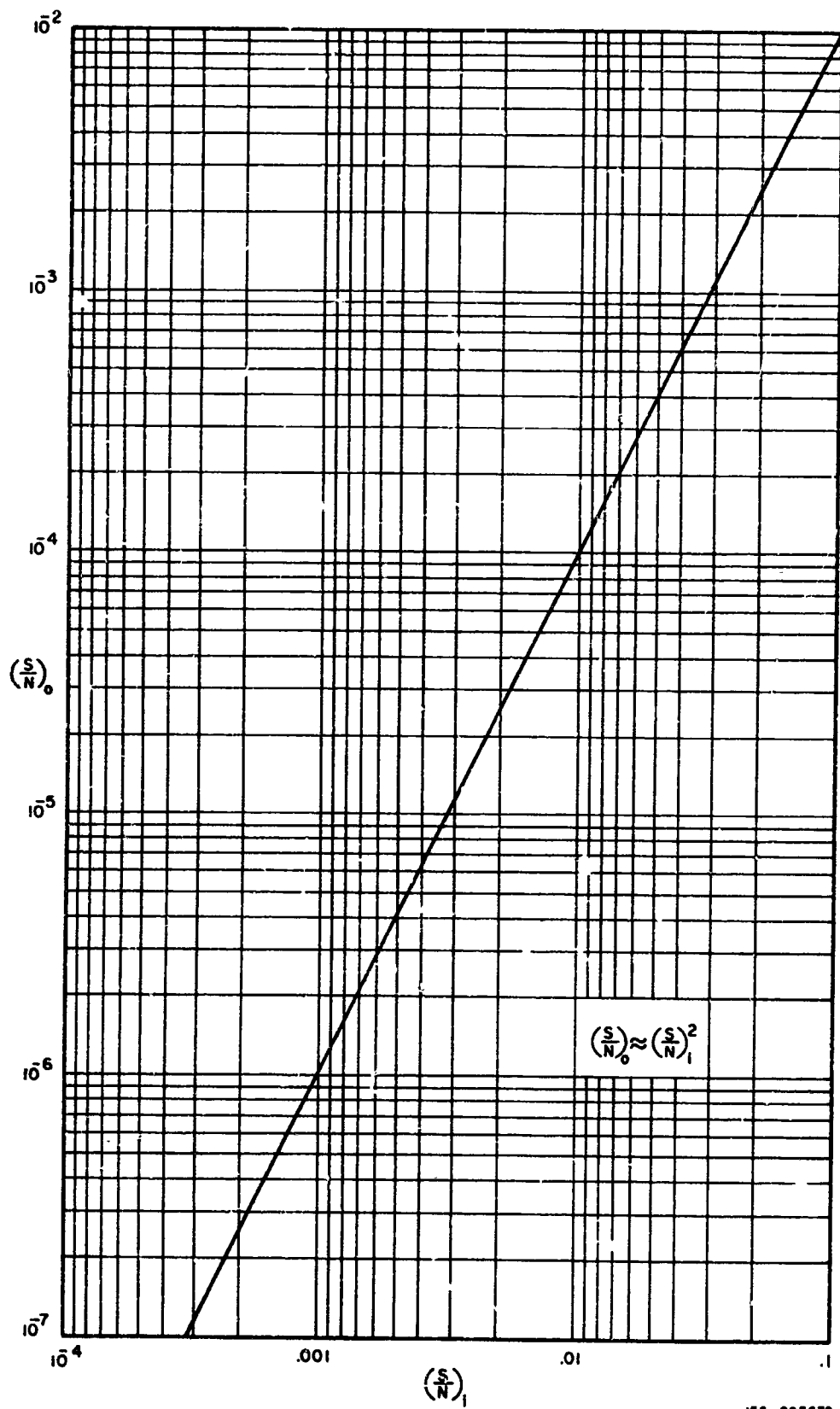


Figure 8. Output versus Input Signal to Noise Ratio

With coherent detection, the output signal-to-noise ratio is equal to the input signal-to-noise ratio:

$$s_o/n_o = s_i/n_i \quad (21)$$

since

$$\frac{s_o}{n_o} = \frac{2ars_i}{2arn_i} \quad (22)$$

It is to be noted that both the signal power and noise power are of larger magnitude than before by the factor $2ar$. Thus, although the input SNR did not improve, the process of coherent detection will tend to eliminate the effects of internal noise if $2ar > 1$, since the internal noise is constant.

At optical frequencies, theoretically, at least, r can be made quite large no matter how small s_i , thus eliminating the internal noise from the noise considerations and providing a great deal of conversion gain since the output $2ars_i > s_i$. In a practical case, however, the reference is not a pure sinusoid and if r is much larger than s_i , any noise in r can be significant.

If we express the reference as a sum of pure reference sinusoid r_o plus a much smaller reference noise r_n

$$r = r_o + r_n \quad (23)$$

The component ar^2 which was previously considered constant is equal to

$$ar^2 = a(r_o + r_n)^2 = ar_o^2 + 2ar_or_n + ar_n^2 \quad (24)$$

The first term is a constant and so is of no concern. The third term is negligible, since $r_o \gg r_n$. The second term, $2ar_o r_n$, however, must be considered in equation (20). This gives

$$e_o = 2ar_o(s_i + n_i + r_n) \quad (25)$$

where r is replaced by r_o , since $r_o \approx r$. The expression reveals that the noise r_n in the reference adds directly to the input noise. The SNR for this condition is given by

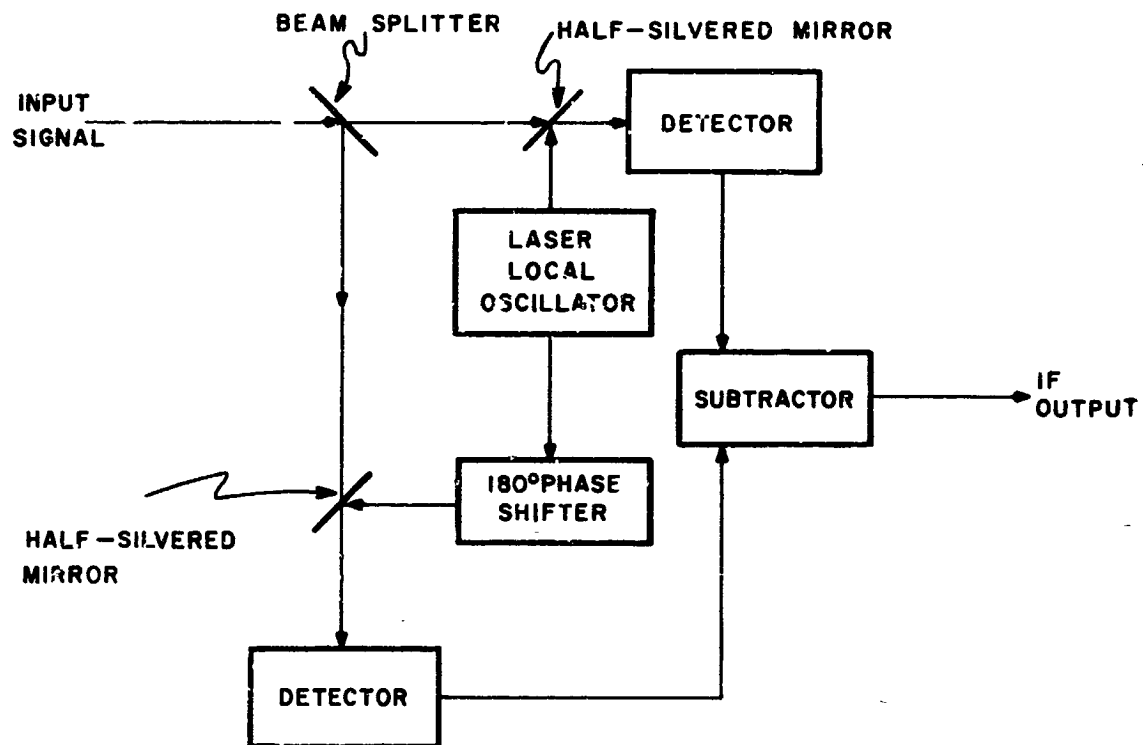
$$\frac{s_o}{n_o} = \frac{s_i}{n_i + r_n} \quad (26)$$

It is clear from the above expression that, assuming one has the purest reference signal obtainable, one can reduce r_n only by reducing r , either through attenuation or use of a lower power reference. However, conversion gain is supplied by the reference signal (since the quantity $2ar_o \gg 1$), and any reduction in r will linearly reduce the conversion gain. It is through the advantage of conversion gain that the internal noise of the photo-detector and background noise is rendered insignificant. Thus, the sensitivity that can be achieved by photomixing is limited by the purity of the local oscillator.

In RF systems, the effect of noise in the local oscillator signal is reduced by use of a balanced detector. The response of a balanced detector is given by

$$e_o = \frac{a}{2} \left[(s_i + n_i + r)^2 - K(s_i + n_i - r)^2 \right] \quad (27)$$

where it is desired that the constant K be close as possible to unity. A balanced detector basically consists of two nearly identical detectors (see Figure 9). The input plus the reference is fed into one detector; the input minus the reference is fed into the other detector. The outputs from the detectors subtract to form the resultant signal. The resultant expression gives



156-005673

Figure 9. Optical Balanced Mixer

$$e_o = \frac{a}{2} \left[2r(s_i + n_i) (1 + K) + (1 - K) \left[(s_i + n_i)^2 + r^2 \right] \right] \quad (28)$$

Introducing the reference noise r_n once again, and noting that $r = r_o + r_n$, $r \approx r_o$, and $r \gg r_n$, we obtain

$$e_o = \frac{a}{2} \left[2r_o(s_i + n_i) (1 + K) + (1 - K) (2r_o r_n) \right] \quad (29)$$

when K is nearly unity, we have

$$e_o = 2ar_o \left[s_i + n_i + \frac{(1 - K)}{2} r_n \right] \quad (30)$$

The above expression indicates that great reduction in reference noise can occur with use of a balanced mixer. At microwaves, balanced mixers have been used with much success for a number of years. Figure 10 plots the noise reduction due to balanced mixer action for various values of K , the factor of matching of detectors, and the ratio of reference noise to reference signal, r_n/r .

Returning to the considerations of coherent detection as an advantage over noncoherent detection, it is clear by using equation (16) and (22) that the loss due to noncoherent detection is given by

$$\text{SNR reduction} = \frac{s_i}{n_i} \quad \text{for} \quad \frac{s_i}{n_i} < 1 \quad (31)$$

When the input SNR is much greater than unity, the noncoherent detection case provides essentially the same performance as coherent detection. This can be seen for noncoherent detection from equation (12), noting that if $s_i \gg n_i$,

$$s_o + n_o \approx a(s_i^2 + 2s_i n_i) \quad (32)$$

Thus, the SNR is given by

$$\frac{s_o}{n_o} = \frac{s_i}{2n_i} \quad (33)$$

A 3 db difference between input and output exists due to the noise beating with the signal. Since it has been assumed s_i/n_i is high, a 3 db difference may not be significant. When considering coherent detection, the effect on the output SNR is independent of the input SNR; that is, for $s_i/n_i \gg 1$, we still obtain

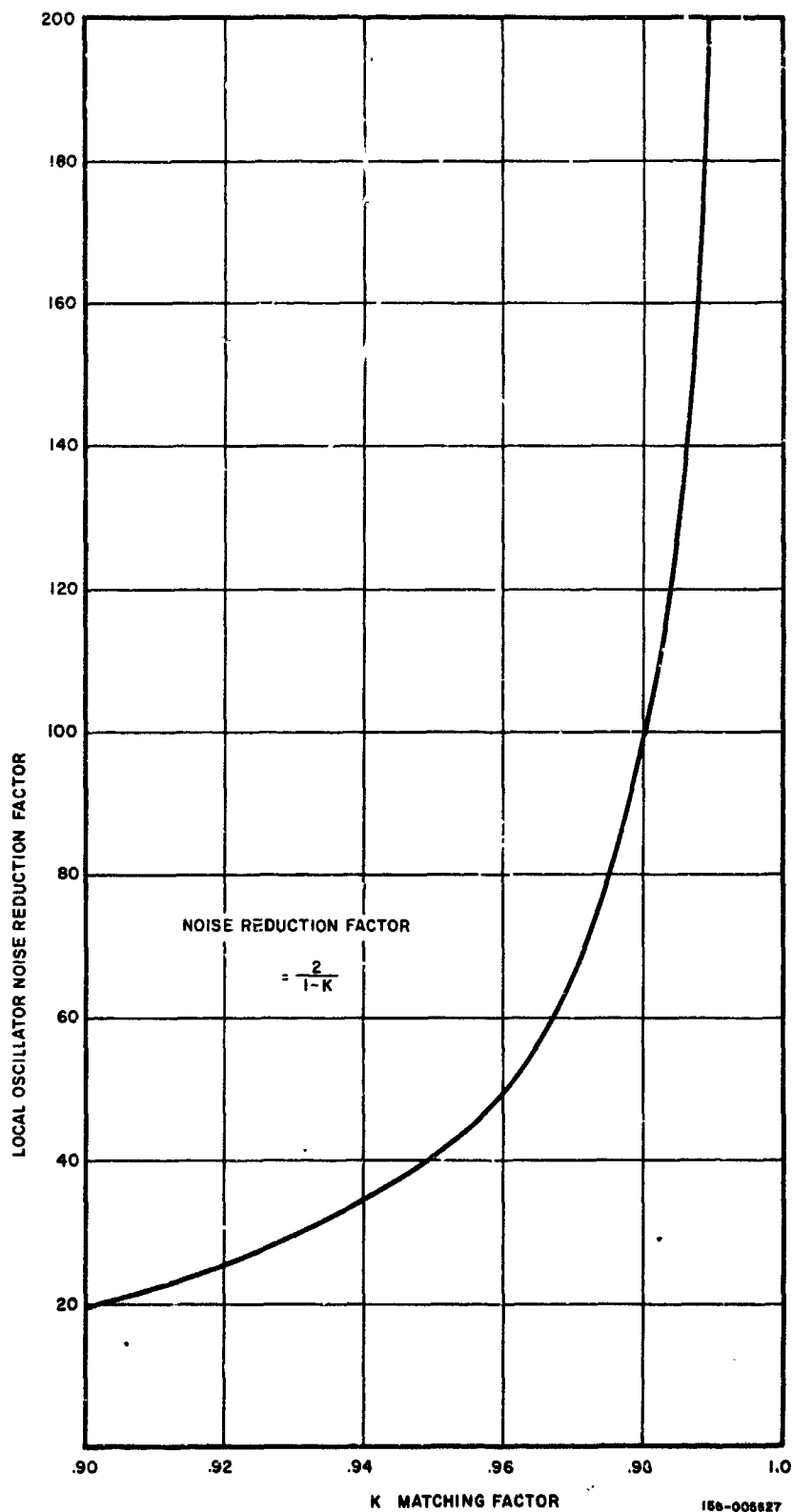


Figure 10. Noise Reduction Due to Balanced Mixer Action for Various Values of K, the Factor of Matching of Detectors, and the Ratio of Reference Noise to Reference Signal r_n/r .

$$\frac{s_o}{n_o} = \frac{s_i}{n_i} \quad (34)$$

Thus, coherent detection will be slightly better than noncoherent detection for high SNR. But, if the SNR is high, it becomes questionable whether the added complexity of coherent detection is worth the small improvement.

Another point to emphasize in this comparison is that in the highest sensitivity case, that of signal photon-limited sensitivity, the SNR must always be greater than unity if one is to communicate over a finite bandwidth; in these cases noncoherent detection is almost as satisfactory as coherent detection.

The foregoing simple analysis of photomixing presented some fundamental considerations of signal, noise and conversion gain in the photomixing process. In the following pages photomixing will be considered in detail, from both the theoretical and practical considerations. The analysis of photomixing is first presented from an electromagnetic wave point of view. (See Ref. 2.)

The field at the photo-sensitive surface is given by

$$E = E_{lo} \cos(\omega_{lo} t) + E_s \cos(\omega_s t) \quad (35)$$

Over a time period much greater than the time period of an optical cycle

$$t \gg \frac{1}{f_{lo}} \approx \frac{1}{f_s} \quad (36)$$

$$\frac{E^2}{2} = \frac{1}{2} E_{lo}^2 + E_{lo} E_s \cos(\omega_{lo} - \omega_s) t + \frac{1}{2} E_s^2 \quad (37)$$

provided certain essential spatial conditions are met which will be discussed later. The resultant alternating component of current from the photo-detector at the difference frequency will be

$$i_{\text{peak AC}} = \frac{2 E_s E_{lo}}{E_{lo}^2 + E_s^2} i_{\text{DC}} \quad (38)$$

If $E_s \ll E_{lo}$, that is, if the local oscillator power is much greater than the incoming signal power, and noting that $\overline{i_{AC}^2} = \overline{i_{\text{peak AC}}^2} / 2$, then

$$\overline{i_{AC}^2} = 2 \left[\frac{E_s}{E_{lo}} \right]^2 i_{DC}^2 = 2 \frac{P_s}{P_{lo}} i_{DC}^2 \quad (39)$$

and for $E_{10} \gg E_s$

$$i_{DC} \approx \frac{eqP_{10}}{hf} \quad (40)$$

Since the shot noise is caused by fluctuations in the average current,

$$\overline{i_n^2} \approx 2qi_{DC}B \quad (41)$$

where B is the detector bandwidth employed. Therefore, assuming a laser local oscillator which generates only shot noise

$$\frac{\overline{i_{AC}^2}}{\overline{i_n^2}} = \frac{2P_s}{P_{10}} \frac{i_{dc}^2}{2qi_{dc}B} = \frac{\epsilon P_s}{hfB} \quad (42)$$

It is to be noted that ideal photomixing is not too different from photo-detection if one considers the signal carrier and sidebands in the direct detection process as equivalent to local oscillator and signal. That is, if one considers an optical carrier frequency, f_c , and a single sideband which is at the frequency $f_c - f_m$ rather than a local oscillator frequency and a signal frequency, the same process occurs in direct detection as in photomixing. However, in direct detection the carrier and sideband powers are both low and of the same order of magnitude, hence the effects are different. With photo-detection the detected currents are of much lower magnitude. Also, the difference frequency is simply the modulation frequency, f_m , which has been recovered. On the other hand, no spatial alignment problem exists because all the energy is coming from one source.

Shot noise in the photomixing process is mainly due to local oscillator power. This follows from the signal and noise multiplication (conversion gain) of photomixing and the fact that the local oscillator power is so much greater than the other powers, including the background. In other words, as long as $P_{10} \gg P_b$, photomixing will discriminate against the background noise that is not at $f_s \pm \frac{B_{IF}}{2}$ where B_{IF} is the bandwidth of the difference frequency,

$f_{10} - f_s$. The ability of photomixing to suppress the background noise, as well as that of internal shot noise is illustrated in Figure 11. Figure 11a shows the signal and the various noise powers with direct detection and Figure 11b shows the influence of the local oscillator power on both signal and noise. In Figure 11b the local oscillator power is only 4 times the original signal power, whereas in practice, it would be many orders of magnitude greater, thereby completely obliterating the impact of the other shot noise sources.

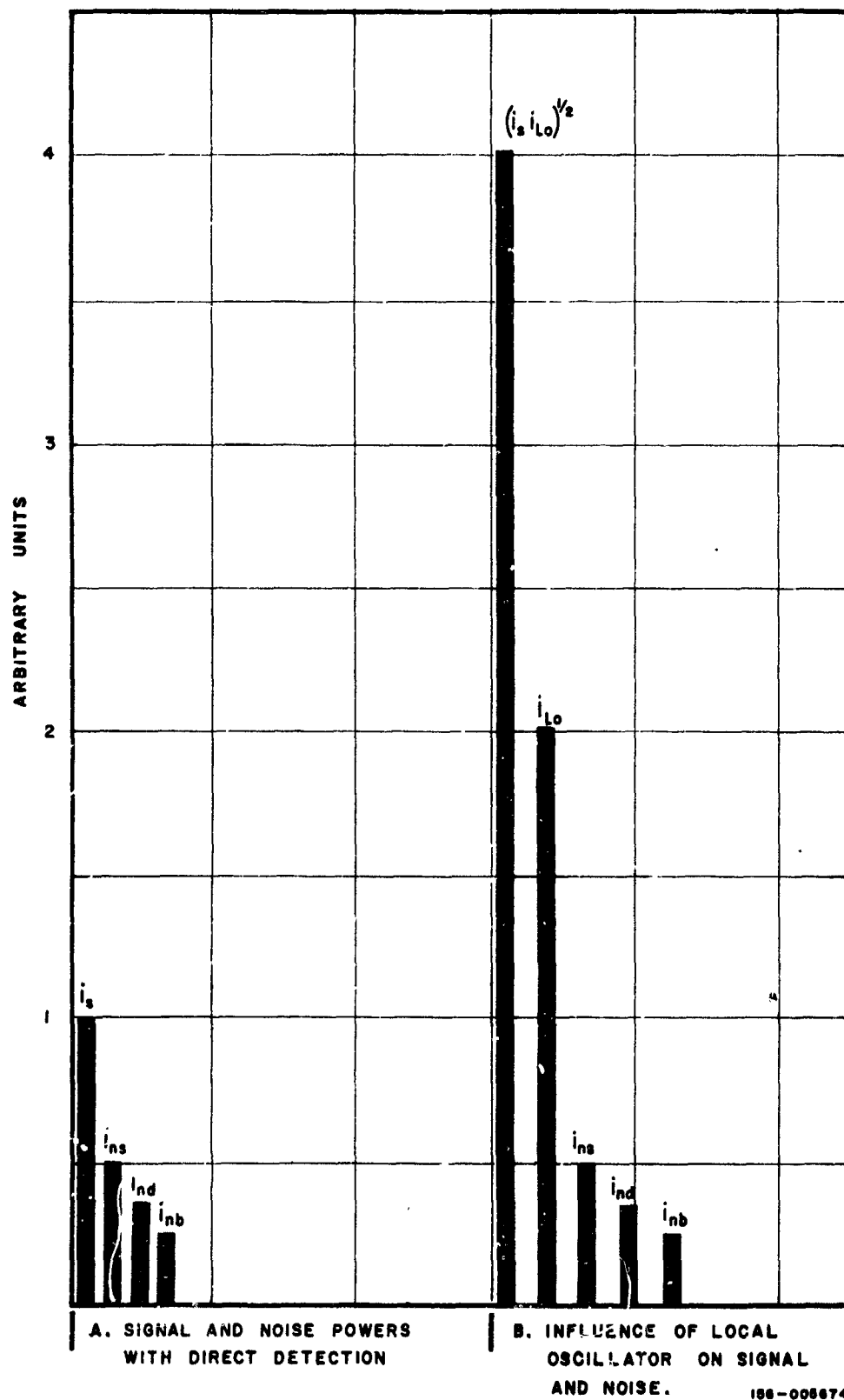


Figure 11. Noise Suppression with Photomixing.

It can be shown that the SNR is given, in general, by

$$\frac{i_s^2}{i_n^2} \approx \frac{\epsilon P_s}{hfB \left(1 + \frac{P_s}{P_{Lo}}\right)} \quad \text{for } P_{Lo} > P_s \quad (43)$$

As P_{Lo} increases, the SNR approaches the limiting value given by Equation (42). As P_{Lo} decreases and P_s/P_{Lo} approaches unity, the SNR approaches that of direct photodetection.

In mathematical terms, for perfect square-law direct photodetection

$$e_o = ae_i^2 \quad (44)$$

For an AM signal with modulation factor, m ,

$$e_i = A_c \left[\cos \omega_c t + \frac{m}{2} \cos (\omega_c - \omega_m)t + \frac{m}{2} \cos (\omega_c + \omega_m)t \right] \quad (45)$$

thus

$$e_o = aA_c^2 \left[\cos^2 \omega_c t + m \cos \omega_c t \cdot \left[\cos (\omega_c - \omega_m)t + \cos (\omega_c + \omega_m)t \right] + \left[\frac{m}{2} \cos (\omega_c - \omega_m)t + \frac{m}{2} \cos (\omega_c + \omega_m)t \right]^2 \right] \quad (46)$$

By expanding and using trigonometric substitution we obtain

$$e_o = aA_c^2 \left[\cos^2 \omega_c t + m \cos \omega_c t + \frac{m^2}{4} \cos^2 (\omega_c - \omega_m)t + m^2 \cos (\omega_c - \omega_m)t \cos (\omega_c + \omega_m)t + \frac{m^2}{4} \cos^2 (\omega_c + \omega_m)t \right]$$

By appropriate filtering of all frequencies above f_m , we obtain

$$e_o = aA_c^2 m \cos \omega_m t \quad (47)$$

Thus, the rms value of the signal voltage is

$$\left(\frac{e^2}{2} \right)^{1/2} = \frac{aAc^2}{2} m \sim P_c m \quad (48)$$

In terms of detected signal current

$$\left(\frac{i_s^2}{2} \right)^{1/2} \sim P_c m = m \overline{i_c} \quad (49)$$

where $\overline{i_c}$ is the average current due to the carrier power.

Thus, the detected signal power is only m^2 of the detected carrier power since

$$\frac{\overline{i_s^2}}{\overline{i_c^2}} = m^2 \quad (50)$$

1.2.1.4 Spatial Requirements of Photomixing

The spatial requirements for photomixing have been shown to be much more severe than for microwave mixing. (Ref. 3.) The basic reason is the optical wavelength is small compared to the photomixing area. Consider Figure 12. Let the signal be denoted as $e_o = E_s \sin \omega_s t$. The local oscillator is given by

$$e_r = E_r \cos (\omega_r - \beta_x) \quad (51)$$

where

$$\beta = \frac{\omega_r}{\nu_x} \quad (52)$$

however, if one examines Figure 12, one recognizes that

$$\sin \theta = \frac{c}{\nu_x} \quad (53)$$

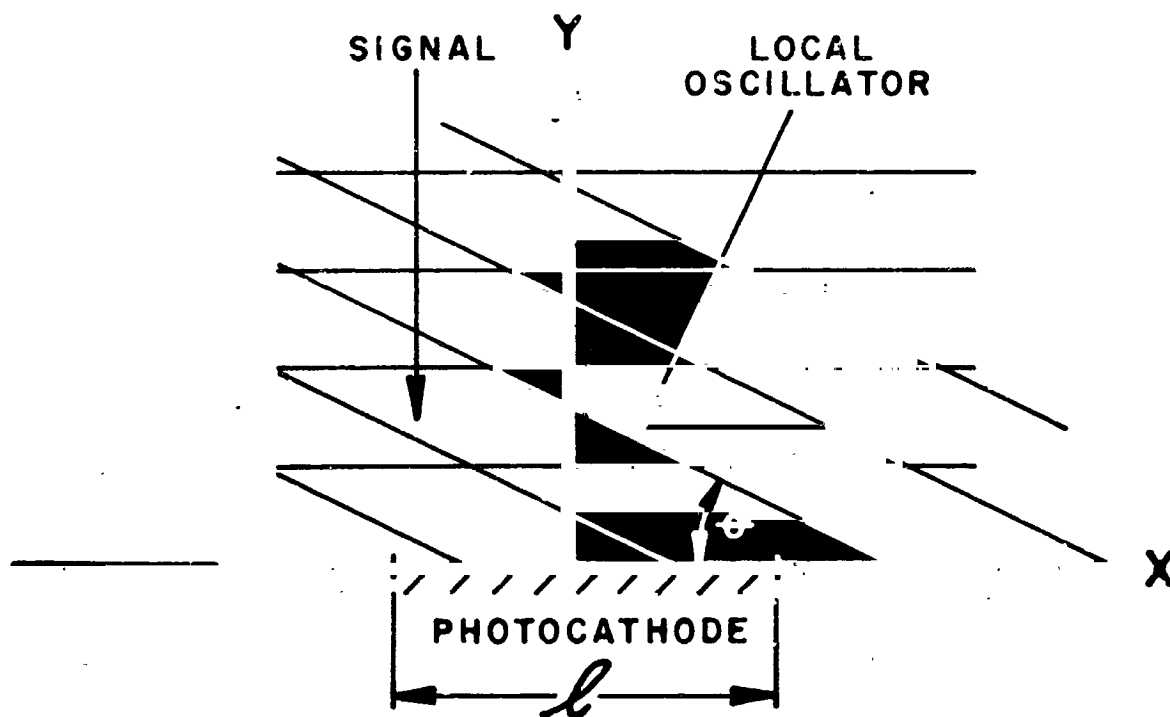


Figure 12. Alignment of Signal and Local Oscillator for Photomixing.

Therefore,

$$\beta = \frac{2 \pi f_r \sin \theta}{c} = \frac{2 \pi \sin \theta}{\lambda_r} \quad (54)$$

The current density is given by

$$\frac{d_i}{d_x} = (e_s + e_r)^2 \quad (55)$$

Expanding the above and dropping terms when the frequencies are greater than ω_r , and noting that $\omega_{IF} = \omega_s - \omega_o$, one obtains the following:

$$\frac{d_i}{d_x} = \frac{E_s^2 + E_r^2}{2} + E_r E_s \cos (\omega_{IF} t + \beta_x) \quad (56)$$

Integrating over the photomixing surface from

$-\frac{l}{2}$ to $+\frac{l}{2}$ we have,

$$i = \int_{-\frac{l}{2}}^{+\frac{l}{2}} \left(\frac{E_s^2 + E_r^2}{2} \right) dx + \int_{-\frac{l}{2}}^{+\frac{l}{2}} E_r E_s \cos (\omega_{IF} t + \beta_x) dx \quad (57)$$

By trigonometric substitution we obtain,

$$i = l \left[\frac{E_s^2 + E_r^2}{2} \right] + E_r E_s \int_{-\frac{l}{2}}^{+\frac{l}{2}} \cos (\omega_{IF} t) \cos \beta_x dx - E_r E_s \int_{-\frac{l}{2}}^{+\frac{l}{2}} \sin (\omega_{IF} t) \sin \beta_x dx \quad (58)$$

Completing integration and evaluating the integral we obtain

$$i = l \left[\frac{E_s^2 + E_r^2}{2} \right] + 2E_r E_s \frac{\cos(\omega_{IF} t) \sin \frac{\beta l}{2}}{\beta} \quad (59)$$

With rearrangement of terms, we can place this in the following convenient form.

$$i = l \left[\frac{E_s^2 + E_r^2}{2} + E_s E_r \cos \omega_{IF} t \left(\frac{\sin \frac{\beta l}{2}}{\frac{\beta l}{2}} \right) \right] \quad (60)$$

It is clear from the above expression if $\beta l \gg 1$, the term involving the difference frequency will be small compared to the direct current terms. The difference term inside the brackets is largest when

$$\frac{\sin \frac{\beta l}{2}}{\frac{\beta l}{2}} = 1 \quad (61)$$

and will start to be reduced substantially when $\frac{\beta l}{2} \gg 1$; however, since

$$\beta l = 2\pi l \frac{\sin \theta}{\lambda_L} \quad (62)$$

it can be seen that for βl to be small (two or less)

$$\sin \theta < \frac{\lambda_L}{\pi l} \quad (63)$$

Since λ_L is the order of 10^{-4} cm and l will be about one cm on a normal photocathode or photosurface, it follows that

$$\frac{\lambda_L}{\pi l} < 10^{-4} \quad (64)$$

Thus, since $\sin \theta \approx \theta$ for small angles, θ must be less than 10^{-4} in order not to reduce the term involving the difference frequency.

The stringent spatial requirements on photomixing given above lead to serious practical problems in a receiver system which differ considerably from the use of photomixing as an experimental laboratory tool. These practical problems are dealt within the material pertaining to systems.

One method that would appear to reduce the spatial requirements is use of the Airy disk principle. (Ref. 4) Consider Figure 13.

The developed method is based on the fact that at the focus of a diffraction-limited lens or mirror, the wavefront in the Airy disk appears to be plane and perpendicular to the direction of the incident light. When the signal beam is focused to a diffraction-limited spot and when a collimated local oscillator beam is also imposed on the spot, then photomixing can take place.

Experimental evidence has been forthcoming and is shown in Figure 14, along with the theoretical curve. Figure 13 shows the photomixing configuration. An aperture larger than the diameter of the Airy disk is used to block the unused portion of the local oscillator beam from entering the photo-detector. The majority of the local oscillator beam is wasted, since the active area over which photomixing can take place is simply the area of the Airy disk. Since the remainder of the local oscillator beam would not contribute to the photomixing action, it is important to prevent it from entering the photo-detector in order to reduce the shot noise due to the local oscillator. This aperture must be correctly positioned to within a fraction of its diameter, and thus involves careful mechanical alignment.

The disk diameter is determined by $\lambda F/D$, where F is the focal length and D the diameter of the lens. To have no significant decrease in the photomixing difference frequency term, it is known that

$$\theta < \frac{\lambda}{\pi \ell} \quad (65)$$

However, in the previous case ℓ was the complete photomixing surface, it is now the disk diameter, d . Thus, $\theta < \frac{\lambda}{\pi d}$. It follows that the allowed angular tolerance is given by

$$\theta < \frac{D}{\pi F} \quad (66)$$

In the first experiment with an Airy disk, the focal length of the focusing lens was 60 cm and the effective lens diameter was 4 millimeters. The disk diameter, d , was thus calculated to be about .10 mm (from $d = \lambda F/D$, $\lambda = .63$ microns). Experimentally, .19 was measured. The tolerance in angular alignment, θ , is calculated to be .12 degrees or .0021 radians. (The theoretical curve shown in Figure 14 is based on the actual spot diameter .19 mm.) With an increase in the D/F ratio, the angular requirements for photomixing are further eased. With a collecting lens of 10 cm, for example, the angular tolerance becomes 3 degrees. The spot diameter, d , however, has been reduced to .004 mm, which will present other problems such as alignment of the aperture and high power density effects on the photosurface. A power input of 10^{-3} watts, for example, over .004 mm diameter is a power density of approximately 600 watts/cm². This will induce heating, photocathode fatigue, and other detrimental effects.

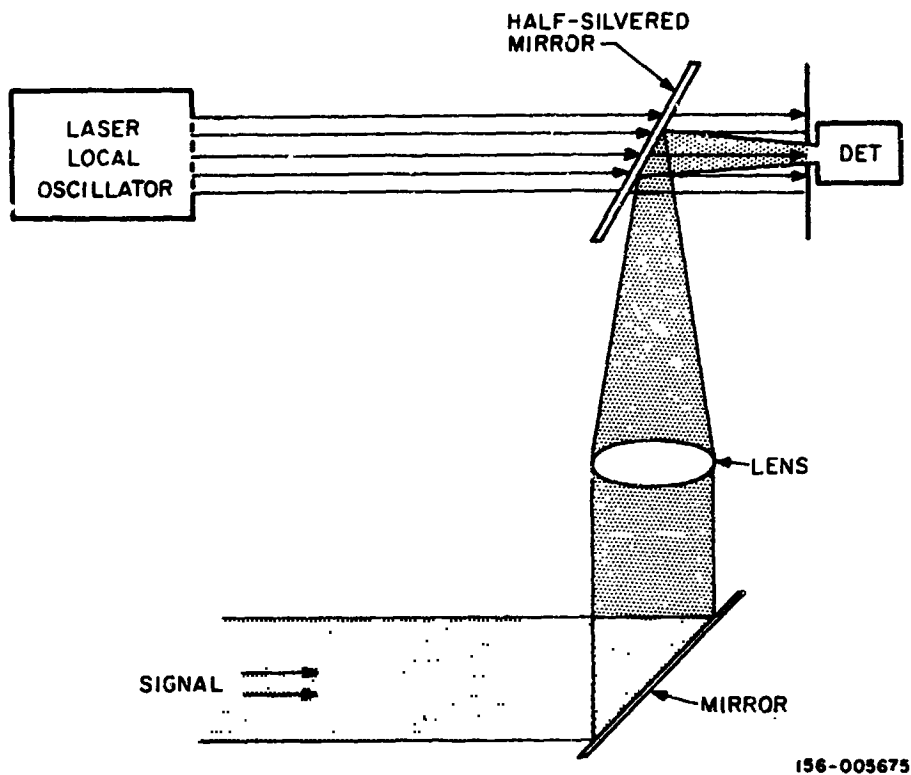


Figure 13. Airy Disk System for Less Critical Angular Alignment for Photomixing

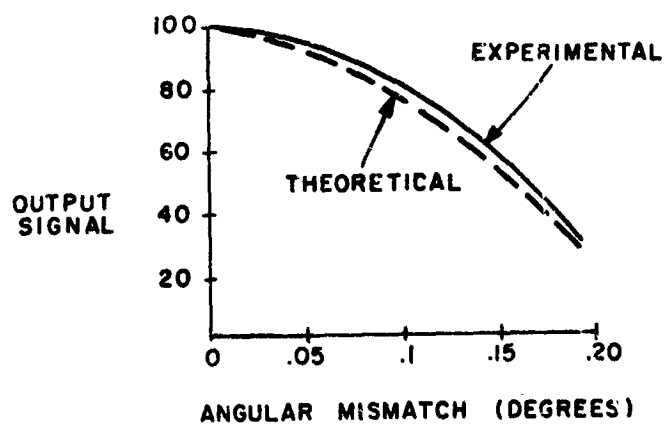


Figure 14. Detected Output vs. Angular Mismatch

1.2.1.5 Local Oscillator Power Requirements

If less conversion gain is required in the photomixing process, the incident power requirements can be reduced. With lower conversion gain required by the photomixing process there will be less effective local oscillator power required. This in turn will reduce the relative local oscillator noise contribution. As discussed earlier, the local oscillator noise can degrade the input SNR considerably. By reduction of the local oscillator power to values not too much greater than the minimum detectable signal power calculated from quantum considerations, one can considerably negate the influence of the local oscillator noise. However, the lack of large conversion gain will lead to the internal detector noise being significant unless sufficient low noise post detection gain is provided. A photomultiplier provides essentially noiseless post-detection gain and so can simplify the photomixing technique by easing the noise requirements of the local oscillator. The post-detection gain of the photomultiplier will be equivalent to the conversion gain of the photomixing process if the background power and the dark current shot noise are of sufficiently low relative value as to not contribute significantly to the total noise. A major advantage of photomixing with high conversion gain lies in the ability to make the noise contributions of the background and the internal device negligible. It is clear, therefore, that the conversion gain cannot be made too low or these advantages are negated. Yet, if the conversion gain is larger than necessary, additional local oscillator noise is introduced. An approximate analysis follows, which arrives at a relationship for determination of the desired value of effective local oscillator power to render the noise contributions of the background and internal shot noise negligible.

The SNR at the detector output is given by

$$\frac{i_s^2}{i_n^2} \approx \frac{(i_{lo} i_{si})}{2qB_{IF}(i_d + i_b + i_s)} \quad (67)$$

where B_{IF} is the IF bandwidth, i_d the dark current; i_b the average current due to background, i_{lo} is the average current due to the local oscillator power, and i_{si} is the average current due to the input signal power.

The following treatment will be used to arrive at a relationship which makes the dark current and background noise negligible. The signal to background noise ratio is given as

$$\frac{i_s^2}{i_{nb}^2} \approx \frac{\left(\frac{\epsilon q P_{lo}}{hf} \right) i_{si}}{2qB_{IF} \frac{\left(\frac{\epsilon q P_b}{hf} \right)}{hf}} \approx \frac{P_{lo}}{P_b} \cdot \frac{i_{si}}{2qB_{IF}} \quad (68)$$

Since $i_{si_MIN} = q(2B_{INF})$ where B_{INF} is the information bandwidth, then

$$\frac{i_s^2}{i_{nb}^2} \approx \frac{P_{Lo}}{P_b} \cdot \frac{B_{INF}}{B_{IF}} \quad (69)$$

If the output signal power is to be considerably greater than the background noise power then,

$$\frac{i_s^2}{i_{nb}^2} > 100 \quad (70)$$

It follows that

$$P_{Lo} \approx 100 P_b \left(\frac{B_{IF}}{B_{INF}} \right) \quad (71)$$

Since B_{IF}/B_{INF} will always be unity or greater, it can be seen that the minimum effective local oscillator power will be at least one hundred times the background power.

It is of interest that the quantum efficiency does not enter in the relationship determining the necessary local oscillator power to dominate the noise due to the background. This is because both local oscillator and background power influence the output signal power and resultant background noise power in a square root fashion. (It remains true, of course, that the minimum input signal power requirements are a function of the quantum efficiency). Similar to the previous development, the signal to dark current noise ratio is determined as

$$\frac{i_s^2}{i_{nd}^2} = \frac{i_{Lo} i_{si}}{2q B_{IF} i_d} \quad (72)$$

and, therefore, for $i_s^2 > 100 i_{nt}^2$,

$$i_{Lo} = 100 i_d \left(\frac{B_{IF}}{B_{INF}} \right) \quad (73)$$

and

$$P_{Lo} \approx \frac{hf}{\epsilon q} \left(\frac{B_{IF}}{B_{INF}} \right) (100 i_d) \quad (74)$$

Since the magnitude of hf/q is on the order of unity, we obtain

$$P_{Lo} \approx \frac{1}{\epsilon} \left(\frac{B_{IF}}{B_{INF}} \right) (100 i_d) \quad (75)$$

In this case, the required local oscillator power is dependent upon the quantum efficiency. In photomultipliers where i_d is small, the quantum efficiency is substantially less than unity; in other detectors i_d is much larger and the quantum efficiency is closer to unity.

Sufficient conversion gain must be provided to dominate the output thermal noise power if use of the laser local oscillator is to result in the best possible signal sensitivity.

The detected local oscillator current is given by $i_{Lo} = \epsilon q P_{Lo} / hf$. If the signal output is to be sufficient, then

$$(i_s i_{Lo}) R \gtrsim 10 kTB$$

Using $i_{smin} = q(2B)$, the necessary local oscillator power is

$$P_{Lo} \geq \frac{5 kT (hf)}{q^2 (R) \epsilon}$$

If the difference or IF frequency is in the microwave region, R can be considered to be 50 ohms. Thus,

$$P_{Lo} \geq \frac{.1 kT (hf)}{q^2 \epsilon}$$

For $f = 3 \times 10^{14}$, $T = 300^\circ K$ and $\epsilon = 1$, $P_{Lo} \geq 3$ milliwatts

If the IF bandwidth is sufficiently narrow to permit conjugate matching, the equivalent R may be higher. This would reduce the local oscillator requirements substantially.

Because of the doppler shift, the IF bandwidth may be required to be considerably wider than the information bandwidth. The effective thermal noise bandwidth is given by

$$B_N = \sqrt{2B_{IF}B_D}$$

where B_D is the post-detection bandwidth is equal to the signal bandwidth. Since the thermal noise bandwidth is effectively increased, the local oscillator power requirements will also increase. As an example, for $B_D = 10$ KC and $B_{IF} = 200$ MC, the effective thermal noise bandwidth has increased to 2 MC. The local oscillator requirements are given by

$$P_{LO} > \frac{5 K T h f}{e_q^2 R} \left(\frac{B_N}{B_D} \right)$$

The importance of the doppler shift on the local oscillator power requirements can be noted from the previous example where $\epsilon = 1$, $f = 3 \times 10^{14}$ cps, and $T = 300^\circ\text{K}$. In that example P_{LO} was at least 3 milliwatts. In the present case $P_{LO} > 600$ milliwatts.

1.2.1.6 Present Status of Photomixing

Photomixing has been successfully achieved under laboratory conditions. However, no operational receiver incorporating photomixing has yet been announced.

One of the practical problems of photomixing is that it requires a stable light source for the local oscillator and carrier. The present laser or quasi-laser devices have too broad a spectrum to qualify, with the exception of the He-Ne type and possibly the ruby laser. The line width of the coherent gallium arsenide diode is about 8 Angstroms, which corresponds to about 3×10^{11} cps. Any modulation frequency less than the latter number will be lost in the self-beats and cross beats of the local oscillator spectrum components and the carrier spectrum. Even with a monochromatic carrier and distinct side bands present, upon entering a photomixing receiver the self-beats between the local oscillator will include the modulation or intermediate frequency and constitute strong interference. The ruby laser line width can be somewhere between 10 to 100 mcs. This could permit microwave modulation in photomixing but would restrict its use at lower modulation frequencies.

The He-Ne laser line width can be expected to be less than 1 mcs., and measurements of much less than 1 kcs have been recorded. It is thus a useful candidate for photomixing, except for the power output problem. The power output is certainly sufficient for local oscillator use, but, to have a carrier at the same or almost the same frequency, the He-Ne laser must also be used as the transmitter. This is mandatory if the output frequency difference after photomixing is to be in the microwave range, or at a lower frequency, since no

other narrow line width laser type is available at the He-Ne laser frequency. The He-Ne gas laser is a low power device and thus its usefulness in communications and radar as a transmitter becomes limited. It is quite possible, however, for an oscillator-amplifier laser transmitter to be used. The laser amplifier is of high power and inherent broad spectrum, but when driven by a narrow input spectrum oscillator, high power over a narrow band results.

Another practical problem in photomixing is frequency control of the local oscillator. It is desirable to vary the optical frequency a small percentage (equivalent to microwave or less frequency shifts) through AFC or some other non-manual and rapid means. One reason for this is to correct for doppler shift, which can be considerable in space applications. Other systems requiring electronic frequency control are high velocity resolution systems and FM systems.

Presently, there are several methods of varying the laser frequency by non-manual means that are rapid enough for inclusion in a receiving system. The amount of shift one can achieve is limited by the method employed. The basic methods utilized are also capable of use for frequency modulation.

1.2.1.7 Some Comparisons between Photomixing and Direct Photo-Detection

It is clear that there will be many considerations involved in the basic choice of specific receiving techniques for a particular application. It would be fruitful to present some fundamental comparisons between photomixing and direct photo-detection with the realization that any judgement must be made on the merits of a comparison for a particular use. Table 1 is a summary of the comparison.

The first elemental difference is that photomixing requires a laser local oscillator. In some radar-like systems, where transmitter and receiver are at the same physical location, it may be possible to utilize the same device as both transmitter source and local oscillator. In communication systems, however, it is clear a laser must be used in a photomixer receiver, whereas one is not necessary in direct photo-detection. Use of a laser local oscillator requires all the considerations discussed earlier to avoid additional noise and interference; that is, a stable narrow line width source is necessary.

Another requirement of photomixing, not required of direct photo-detection, is that the local oscillator energy must arrive at the photomixing surface in spatial phase with the signal energy. This practical requirement becomes quite difficult and must be a part of the comparison if more than laboratory operation of the system is considered.

TABLE I. COMPARISON BETWEEN PHOTOMIXING AND PHOTO-DETECTION

<u>PHOTOMIXING</u>	<u>PHOTO-DETECTION</u>
Needs Laser local oscillator.	No local oscillator required.
Spatial phasing requirements (superposition)	No spatial phase problem.
Expected doppler shifts requires wide optical bandwidth and causes IF problems.	Expected doppler shifts only requires wider optical bandwidth.
Phase distortion limits effective receiver area.	Restriction several orders of magnitude less severe (effective receiver areas can be built much larger).
3 db less noise (hfb) theoretically possible than in photo-detection.	Minimum noise 2 hfb.
Large conversion gain possible with no decrease in input S/N ratio.	Post-detection secondary emission multiplication with no decrease in input S/N ratio current gains of 10^5 to 10^6 .
Background directional and frequency discrimination without use of optical filter.	No frequency discrimination in photo-detection without use of optical filter. Additional directional discrimination with optical filter.
Subject to media disturbance of coherence.	Does not depend on coherence.

This requirement, in turn, puts constraints on the size of the photon collecting area, i.e., the maximum dimension of the lens or parabolic mirror. Optical techniques will restrict the receiver lens or reflecting parabola to the size at which phase distortion begins to become appreciable. That is, when the path lengths from points on the collection area to the photocathode become significantly different (on the order of the wavelength of the optical frequency), spatial phase coincidence with the local oscillator will be lost and rapid deterioration in photomixing performance will occur. Note, however, that the photo-detection technique has its limitations not at the optical frequency but at the modulation frequency, thereby, allowing the use of lenses or parabolic mirror to build an effective receiver area several orders of magnitude greater. Thus, for systems in which large collecting areas are possible, photo-detection offers the ability to gather more useful photons.

The possible large doppler shift at optical frequencies can present serious problems in a photomixing system subject to large velocity changes. As the radial component of velocity changes, the doppler shift frequency

changes, causing a different difference frequency. Possible solutions are to have the IF extremely broad (or tunable over a broad range), or to have the laser local oscillator tunable over the necessary range. Microwave broadband amplifiers are of one octave or less and tunable microwave amplifiers cannot readily be tuned more than one octave. It is also complex and difficult to tune the local oscillator a number of gigacycles per second.

It has been shown that doppler shifts above 30 gigacycles/second will occur in space applications. The doppler shift is given by:

$$f_{DS} = \frac{(C + V)}{(C - V)} \frac{2V}{C} f_L \quad (76)$$

where V is the radial velocity and f_L is the carrier frequency. It can be seen that for a carrier frequency, f_L , of 3×10^{14} cps that

$$f_{DS} = 2 \times 10^9 V \quad (77)$$

where V is in units of kilometers per second and f_{DS} is in units of cps.

In many cases it is likely that the change in the doppler shift frequency will not be rapid and, therefore, slow tuning, possibly even manual tuning, may be sufficient to keep the difference frequency signal within the IF bandwidth. The optical bandwidth of the photomixing system will have to be wide enough to accommodate the range of the doppler shifted frequencies. A signal at 3×10^{14} cps that can be doppler shifted 10 gc/s must have an optical bandwidth of 10 gc/s, although, if tuning is accomplished, the post-mixing or IF bandwidth can be small. If tuning is not employed, then the post-mixing or IF bandwidth must be wide: this will increase the noise.

From a theoretical viewpoint, direct photodetection requires the same optical bandwidth as photomixing. In practice, because there are no filters available which can give the spectral filtering one achieves with photomixing, the optical bandwidth of photodetection receivers are much wider than photomixing receivers. This fact, along with the fact that no difference frequency is necessary, results in photodetection essentially being unaffected by the doppler shifts. That is, the change in optical frequency due to very high radial velocity is still so small a percentage change of the optical frequency that it is unlikely that any difference in receiver response will occur. This is not true if a quantum amplifier is placed before the photodetector. The quantum amplifier is a narrow band device and the doppler shift may be significant enough to result in the shifted optical frequency being outside the optical frequency response of the quantum amplifier.

Photomixing does provide a great deal of background discrimination, both spectral and directional. Spectral discrimination is achieved since only the noise components that fall within the IF bandwidth are amplified. Since the IF bandwidth with photomixing is many times less than the optical bandwidth, and since the optical bandwidth determines photodetection background noise, a

large background noise advantage is possible with photomixing. Consider that a narrow optical filter may be 7 Angstroms wide (about 4×10^{10} cps) whereas the IF bandwidth may in some cases be only 1 mc/s. A reduction in background energy is achieved by the ratio of

$$\frac{B_{\text{opt}}}{B_{\text{IF}}} = \frac{4 \times 10^{10}}{10^6} = 4 \times 10^4 \quad (78)$$

Since the shot noise current due to the background is a function of the square root of the background power (other factors constant such as post-detection bandwidth), a reduction in background noise current of 200 (or 23 db) can be realized in the above example. In general, the background noise current improvement is given by

$$\frac{\left(\frac{i_{\text{nb}}}{P_M} \right)}{\left(\frac{i_{\text{nb}}}{P_D} \right)} = \sqrt{\frac{B_{\text{opt}}}{B_{\text{IF}}}} \quad (79)$$

where $(i_{\text{nb}})_{P_M}$ is the noise current due to the background in a photomixing receiver and $(i_{\text{nb}})_{P_D}$ is the background noise current in a photo-detection receiver. The above assumes $P_{I0} \gg P_b$.

Directional discrimination is achieved by the same mechanism that requires the local oscillator and signal to be properly aligned. If the incident background energy is not from the same direction as the signal, little or no mixing action will occur between it and the local oscillator. Thus, no components at the difference frequency will appear. The background energy which is not from the proper direction to photomix with the local oscillator will simply increase the detected shot noise. Where $P_{I0} \gg P_b$, this will not be a significant noise contribution.

It is possible to achieve highly directional discrimination by other means than photomixing. Fabry-Perot devices such as the interferometer can give high directional discrimination and can be placed before the photo-detector in a direct photo-detection system. In this case, a passive device is used in place of an active device (local oscillator) to achieve similar results.

1.3 New Technology

There are no reportable items within the meaning of the New Technology Clause of NASA Form 417 (1-63) and Alteration dated November 1963.

1.4 Program for Next Reporting Period

There will be no effort expended on Task I in the next reporting period.

1.5 Conclusions and Recommendations

A detailed analysis of optical receiving techniques has shown that in the general case there is no clear cut superiority of either photomixing or direct photo-detection over the other. Rather, it has been shown that the choice of a specific receiving technique must be determined for a particular application.

Photomixing has advantages of producing a large conversion gain with no decrease in input S/N ratio, of providing directional frequency discrimination without use of an optical filter, and of producing 3 dB less hfB noise (theoretically) than in photo-detection. Disadvantages of photomixing include the need of a laser local oscillator, rigid spatial phasing requirements (alignment), limited receiver photon collection area (due to phase distortion limits), and a wide and/or tunable IF stage to accommodate doppler shifts (which can be above 30 gigacycles/second). A consideration of media disturbance over the transmission path is also required since this can affect coherence.

Advantages of direct photo-detection include post-detection secondary emission multiplication gains of 10^5 to 10^6 with no decrease in input S/N ratio, larger receiver photon collection areas, and simple accommodation of expected doppler shifts. No local oscillator is required and there are no spatial phase problem. Disadvantages include a minimum 2hfB noise 3 db greater than photomixing and the lack of directional and frequency discrimination. Media disturbance effects on coherence need not be considered since photo-detection is not dependent on coherence.

2. TASK II EFFORT

2.1 Introduction

Task II consists of a series of ten lectures each four hours in duration, to be presented by Mr. Monte Ross. The lectures, which are to deal with laser receivers and systems, will include the subject matter of Task I. Five lectures were given in the second quarter. Subject matter was as follows:

1. Radiation Laws and Statistics
2. Noise and Fluctuations
3. Detection Statistics
4. Information Theory Aspects

2.2 Discussion

No lectures were given in the third quarter.

The subject matter for the remaining five lectures will include:

1. Receiving Devices
2. Receiving Techniques
3. Receiving Systems
4. Electro-Optic Devices

2.3 New Technology

There are no reportable items under Task II within the meaning of the New Technology clause of NASA Form 417(1-63) and Alterations dated November 1963.

2.4 Program for Next Reporting Period

The lecture material will be prepared for delivery.

2.5 Conclusions and Recommendations

Five of the ten lectures have been delivered. Subject matter for the entire series of ten lectures will be provided in the form of manuals.

3. TASK III EFFORT

3.1 Introduction

Task III consists of developing and delivering one Dynamic Crossed-Field Electron Multiplying (DCFEM) light demodulator which has a voltage signal-to-noise ratio of 3 DB when detecting 10^{-12} watts of 6321AU radiation with a modulation frequency of 3 KMC and a detection bandwidth of 1 KC.

The device incorporates many desirable features of static multipliers, such as low noise, exceptionally high amplification, and good spectral response; it has the additional advantage of providing wide signal bandwidth and a much simpler cathode and secondary emission structure. It has superior characteristics when compared with other available devices capable of detecting high frequency modulation.

This device is the first photomultiplier with microwave response. It enables use in instrumentation and scientific experiments where pulses of a nano-second or less need to be detected in a sensitive manner.

The DCFEM has linear and stable gain over a wide range of operating conditions and can provide unsaturated outputs exceeding one MA, thereby eliminating the need for post detection amplification.

The high sensitivity and large bandwidth of a microwave-bandwidth photomultiplier results in instrument capabilities not previously possible; its specifications show the feasibility of laser systems for space communications and high-resolution radar.

A schematic diagram of the basic detector configuration is indicated in Figure 15. This figure shows two electrodes incorporated in the high electric field region of a rectangular metal cavity resonant at 3 GC. Typical parameters for this configuration are an inter-electrode spacing of 3 mm, and an electric field intensity in the range of 10^5 to 10^6 volts/meter, providing eight multiplication stages. A microwave pump source of not more than a few watts is needed. The active electrode (secondary emission surface) is Beryllium-Copper, Magnesium Oxide or some other suitable material. A small area (20 mm^2) of the active electrode is covered with a photocathode chosen for the spectral response desired. An external magnet supplies a uniform field of about 500 gauss. The length of the column supporting the pedestal is chosen for either $1/4$ or $3/4$ -wavelength resonance modes. It is to be noted that only three external electrical connections are required in contrast to the ten or more connections commonly required with electrostatic photomultipliers.

The electron multiplication in the detector is realized by providing a region in which there are two spatially uniform crossed fields. In Figure 15 the static magnetic field points out of the plane of the paper, and the microwave electric field lies vertically in the plane. The region is bounded by two electrodes, one active electrode having a high secondary emission ratio, δ , and the other an inactive electrode or pedestal having a δ of less than unity. Incident light on the photocathode produces photoelectrons which are accelerated initially in the positive-x direction during the positive portion of the microwave voltage cycle. However, the magnetic field curves the paths as shown, and during the negative

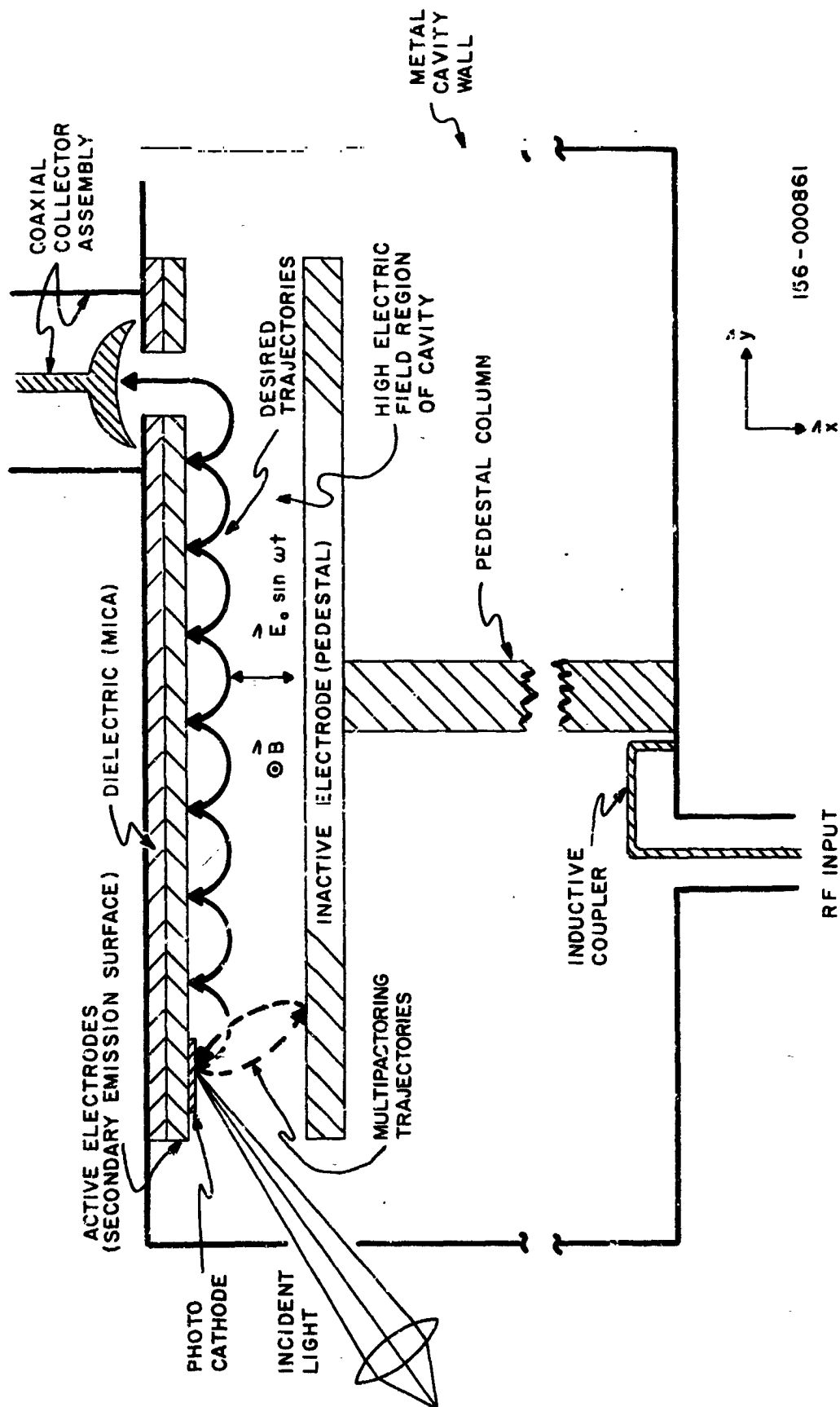


Figure 15. Schematic Diagram of Dynamic Crossed-field Electron Multiplier.

portion of the cycle the electrons impinge back onto the active electrode where they produce secondary emission electrons. Each of these secondaries is accelerated and curved back onto the active electrode, where additional secondaries are produced. This multiplication process is repeated for n stages, after which the electrons are collected by the coaxial collector assembly.

Work in the first quarter determined that for high vacuum purposes it would be an improvement to re-design the cavity in a cylindrical geometry as shown in Figure 16, rather than in a rectangular geometry. This cylindrical geometry is smaller and easier to fabricate, assemble, and align and its electrical characteristics are as good as or better than the rectangular configuration.

Work in the second quarter centered around construction and testing of the cylindrical geometry DCFEM tube shown in Figure 17. Three tubes were constructed and tested: One leaked severely and was discarded; one had a mechanical malfunction and was disassembled for modification; and one tube was operated to obtain preliminary data. Preliminary data from DCFEM tests indicated frequency response to at least 1 KMC/S. Photo-beats up to 600 MC/S have been detected from a gas laser source.

Work in this reporting period, the third quarter consisted of evaluating factors affecting detector life and in obtaining experimental data for DCFEM operation.

3.2 Discussion

3.2.1 Detector Life

A detector was "tipped off" from the pump station in early October 1964 in preparation for delivery to NASA. Although twenty or more detectors had been fabricated in the past, none had ever been removed from the pump station for operation. It was decided that the device could be "tipped off" without resorting to a getters or a small ionization type appendage pump to maintain the proper vacuum. It was reasoned that there was sufficient free cesium remaining in the "tipped off" tube to act as a "getter" under the normal operating conditions of the device.

This premise proved to be true for more than one-hundred hours of operating time. During the last week in November, it was noted that the photo-cathode had deteriorated almost two orders of magnitude in sensitivity. No deterioration of the secondary emission capability was in evidence.

The detector was opened to determine the cause of the failure (This is possible by virtue of integral, high vacuum, flanges as part of these early tubes.) It was noted that the secondary emission surface showed discoloration in the vicinity of the collector indicating excessive oxidation of the beryllium oxide surface. The area where the discoloration was noted is in the normally high electron density region of the device. The vacuum envelope was tested for air leaks, but none were found.

The detector was re-assembled and a new cathode formed. The tube was again tipped off without any getter other than the free cesium remaining in the envelope. This device has been intermittently operated for a period of three weeks and shows no evidence of cathode deterioration.

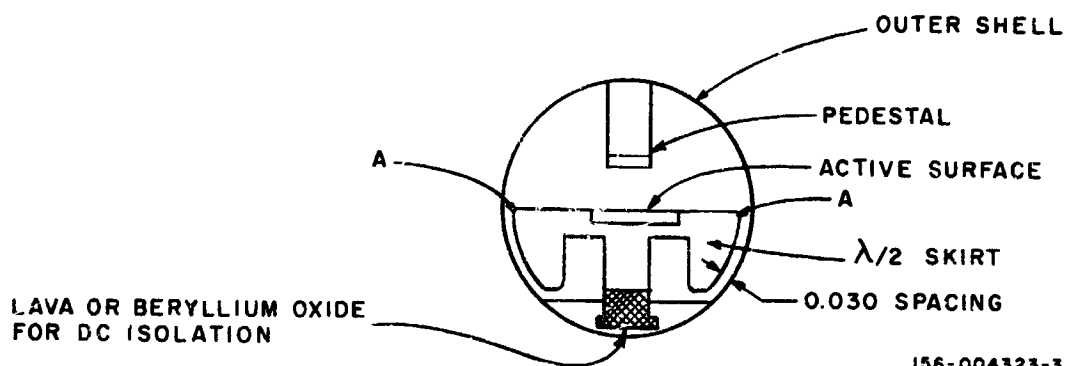


Figure 16. Cylindrical Cavity Using Non-Contacting Microwave Short Circuit.

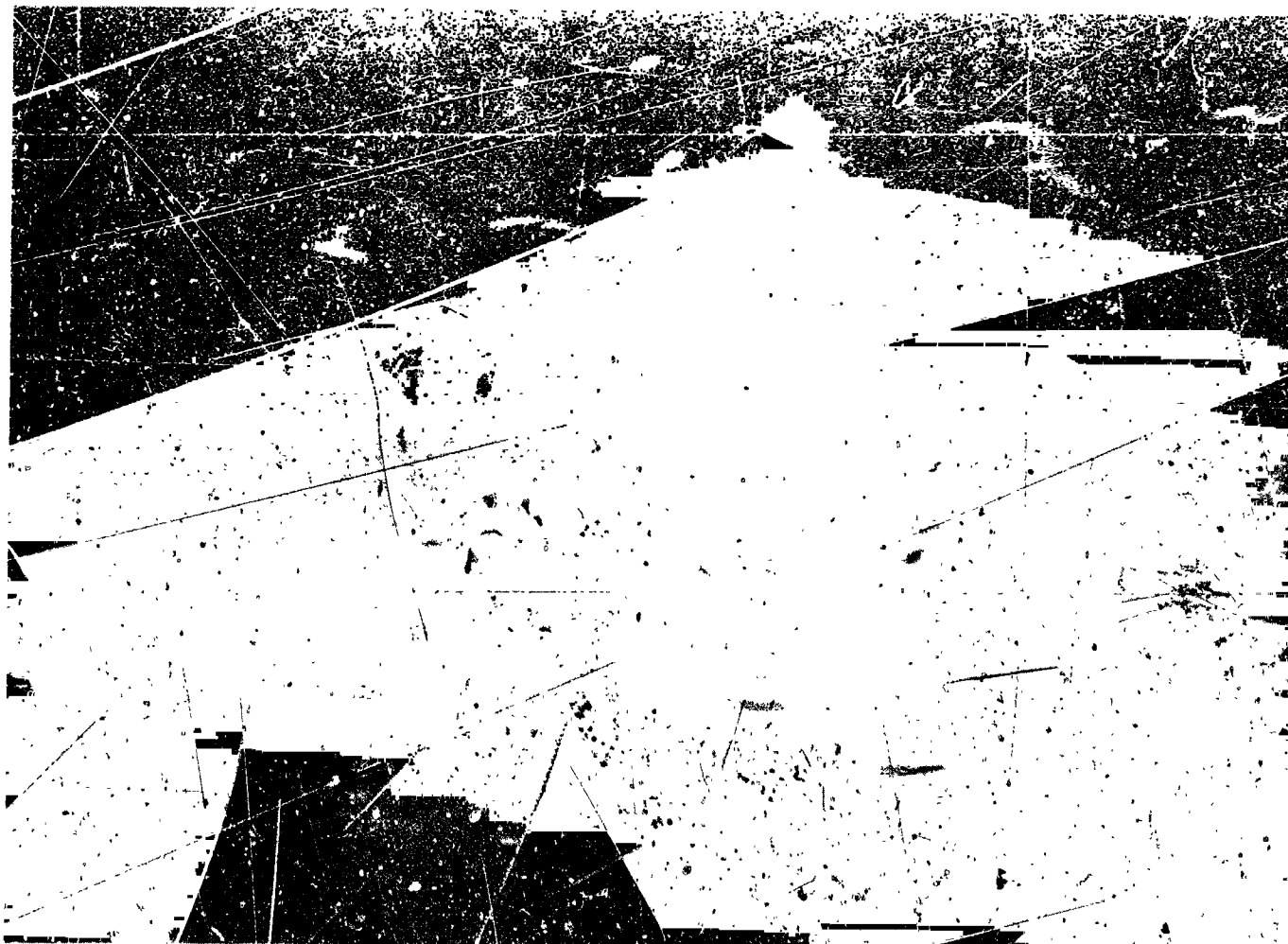


Figure 17. DCFEM (Cylindrical Geometry).

The cause of the cathode deterioration is thought to be due to localized high intensity electron bombardment which produced sufficient internal gassing to eventually oxidize all of the free cesium in the envelope. The intense electron bombardment is due to the previously described phenomena, i.e., multipactoring. This electron instability is known to produce gas in otherwise "clean tubes."

Although present models of the biased DCFEM are much less prone to multipactor, the problem still exists. The detector that eventually failed withstood far more multipactoring than is usual since it was found that judicious alignment of the tube in its external magnet tended to further stabilize it. However, in determining the best position for the tube in the magnetic field, excessive multipactoring was inevitable.

Several steps can be taken to eliminate "softening" of the tube. The most obvious is to eliminate multipactoring altogether. A simpler approach is the use of a small auxiliary ion pump. The ion pump will be used until the detectors are sufficiently stable to replace the pump with a getter.

3.2.2 Experimental Results

Preliminary investigations were made of the gain of the experimental tube as a function of the various tube parameters (electric field, magnetic field, DC bias). Parameters plotted from the experimental data are defined as follows:

I_o = Photo Current (amperes)

I_c = Collected Tube Current (amperes)

Gain = I_c/I_o

B = Magnetic Field (gauss)

ω_c = Electron Cyclotron Resonance Frequency
 $= \frac{eB}{mC}$ radians/second

ω = Tube RF Drive Frequency = 1.97×10^{10} radians/second

$\gamma = \frac{\omega_c}{\omega} = \frac{eB}{mC\omega} = 8.94 \times 10^{-4} B$

e/m = Electron Charge to Mass Ratio

C = Velocity of Light

P_{in} = RF Driving Power (Watts)

VDC = DC Tube Bias (Volts)

Figure 18 shows two cases of gain versus γ . In both cases, $P_{in} = 1.6$ watts and $I_o = 5 \times 10^{-11}$ amps, the difference between cases being the DC bias. In one case the bias remains fixed at 210 volts, whereas in the second curve the bias is adjusted each time for maximum gain. In the region of maximum gain, it can be seen that gain is not seriously affected by optimizing the bias. The maximum difference in gain in this region is less than 1.5:1. Maximum gain occurs at $\gamma = .770 - .790$.

Figure 19 is a plot of gain versus DC bias voltage. All other parameters are constant with $I_o = 5 \times 10^{-11}$ amps, $\gamma = .790$ and $P_{in} = 1.6$ watts. Optimum bias is about 210-220 volts.

Figure 20 shows two cases of current gain versus RF input driving power. This power input is a measure of the RF electric field in the active region of the tube. In one case the DC bias and γ were held constant at the pre-determined maximum points, i.e., VDC = 220 volts and $\gamma = .790$. For the second case, VDC and γ were adjusted for maximum gain at each point. I_o in both cases was 5×10^{-11} amps. It can be seen from this figure that in both cases, the curves are almost collinear, especially in the region of P_{in} from 1.5 to 2.0 watts where the tube appears to operate best. It would appear that variations or fluctuations in DC bias or γ about their optimum points will not seriously affect the gain of the tube; however, it is also obvious that P_{in} (or RF electric field amplitude) does greatly affect gain.

Figure 21 is another plot of optimum gain (VDC and γ adjusted each time) versus power input. These curves, however, show both large and small signal gain, small signal input being $I_o = 5 \times 10^{-11}$ amps and large signals of $I_o = 1 \times 10^{-9}$ amps and $I_o = 1 \times 10^{-8}$ amps. As would be expected, small signal gain is greater than large signal gain: in fact, the curve for $I_o = 1 \times 10^{-8}$ amps appears to reach saturation at P_{in} of about 1.3 watts.

Figure 22 and 23 are plots of optimum DC bias and optimum γ versus P_{in} from the gain curve, Figure 21. It is evident that for both large and small signal gain, these parameters are almost constant in the region of optimum power input ($P_{in} \approx 1.5 \rightarrow 2.0$ watts). However, the optimum values, especially DC bias, vary with the input signal level. Insufficient experimental evidence at the time of this report make it impossible to discuss these optimum parameters versus input current differences with any authority.

Generally, at the small signal level, the tube was very stable and performed well in the region of P_{in} of 1.5 - 2.0 watts. Gain was greatly affected by the driving power level, but two or three percent changes in DC bias and/or γ had little effect on the gain.

3.3 New Technology

There are no reportable items under Task III within the meaning of the New Technology clause of NASA Form 417(1-63) and Alterations dated November 1963.

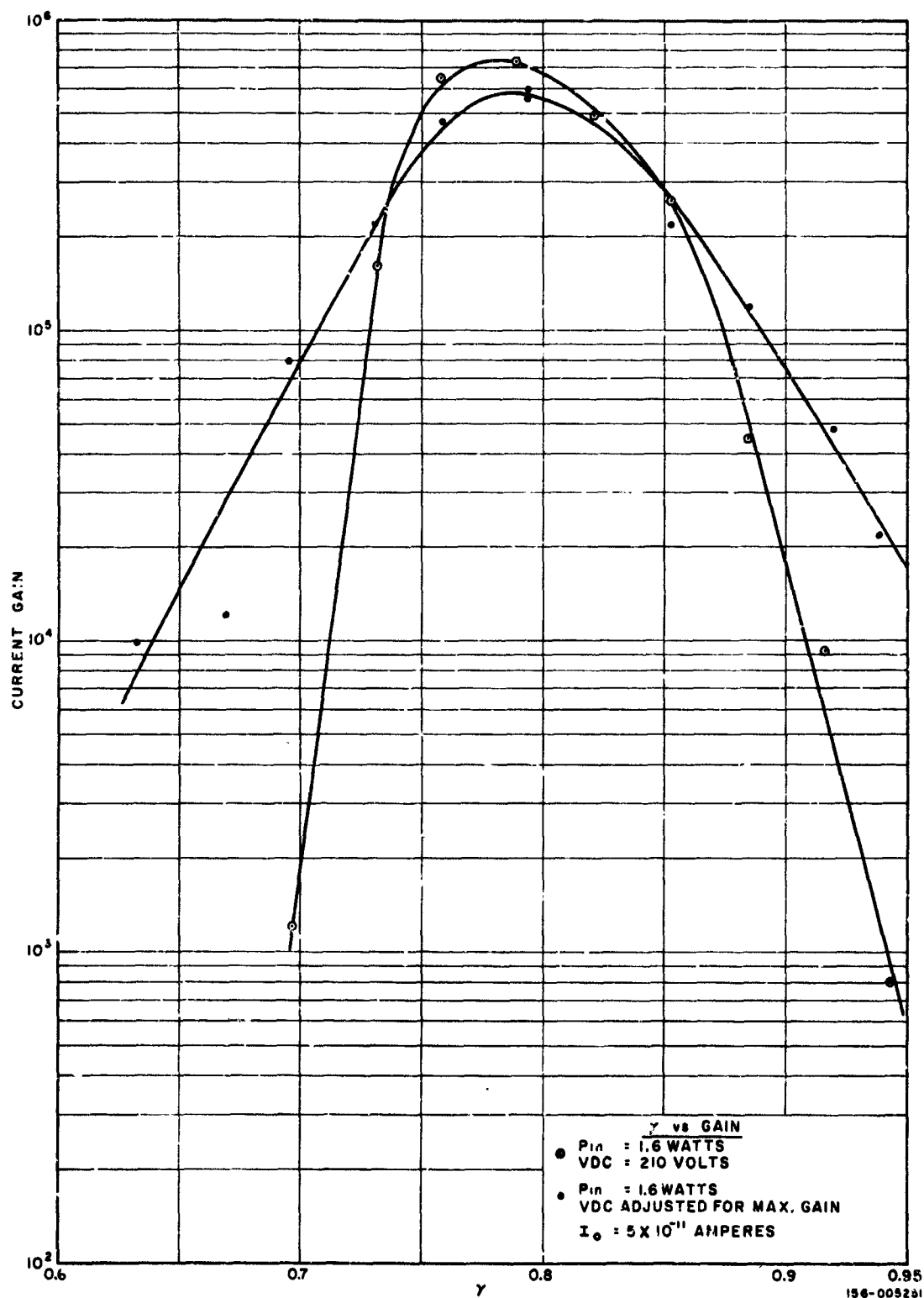


Figure 18. Current Gain vs γ

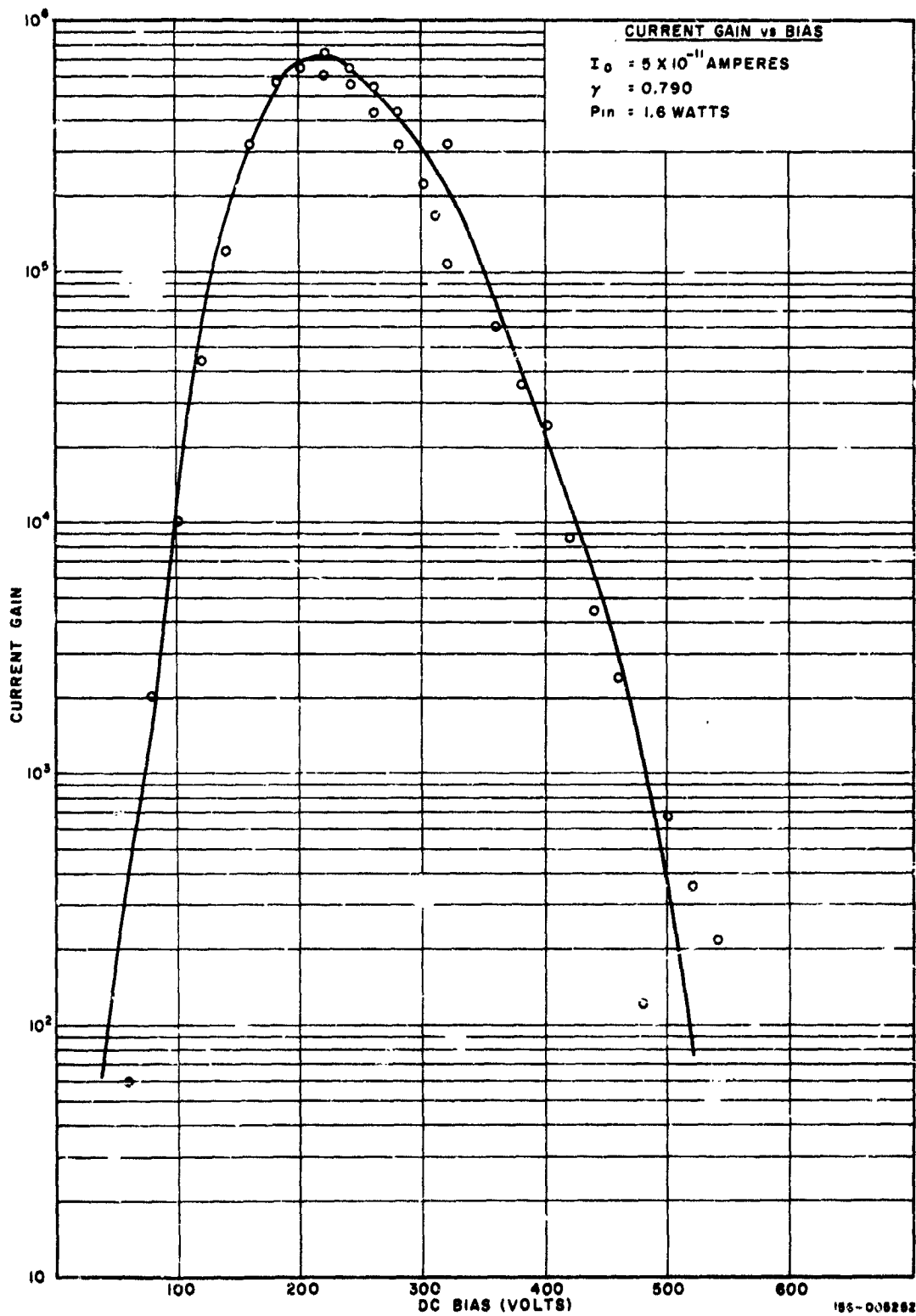


Figure 19. Current Gain vs DC Bias

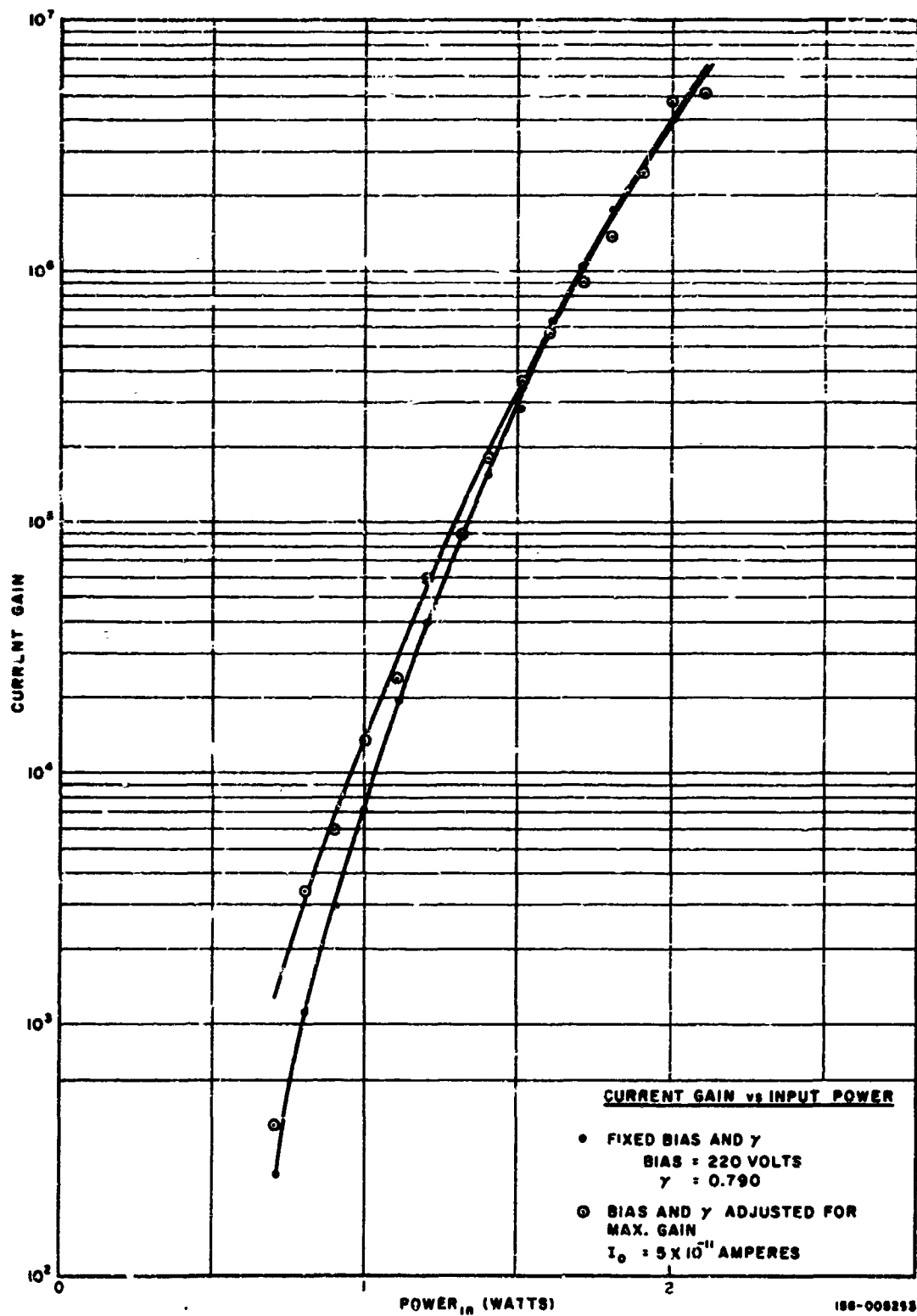


Figure 20. Current Gain vs Input Power

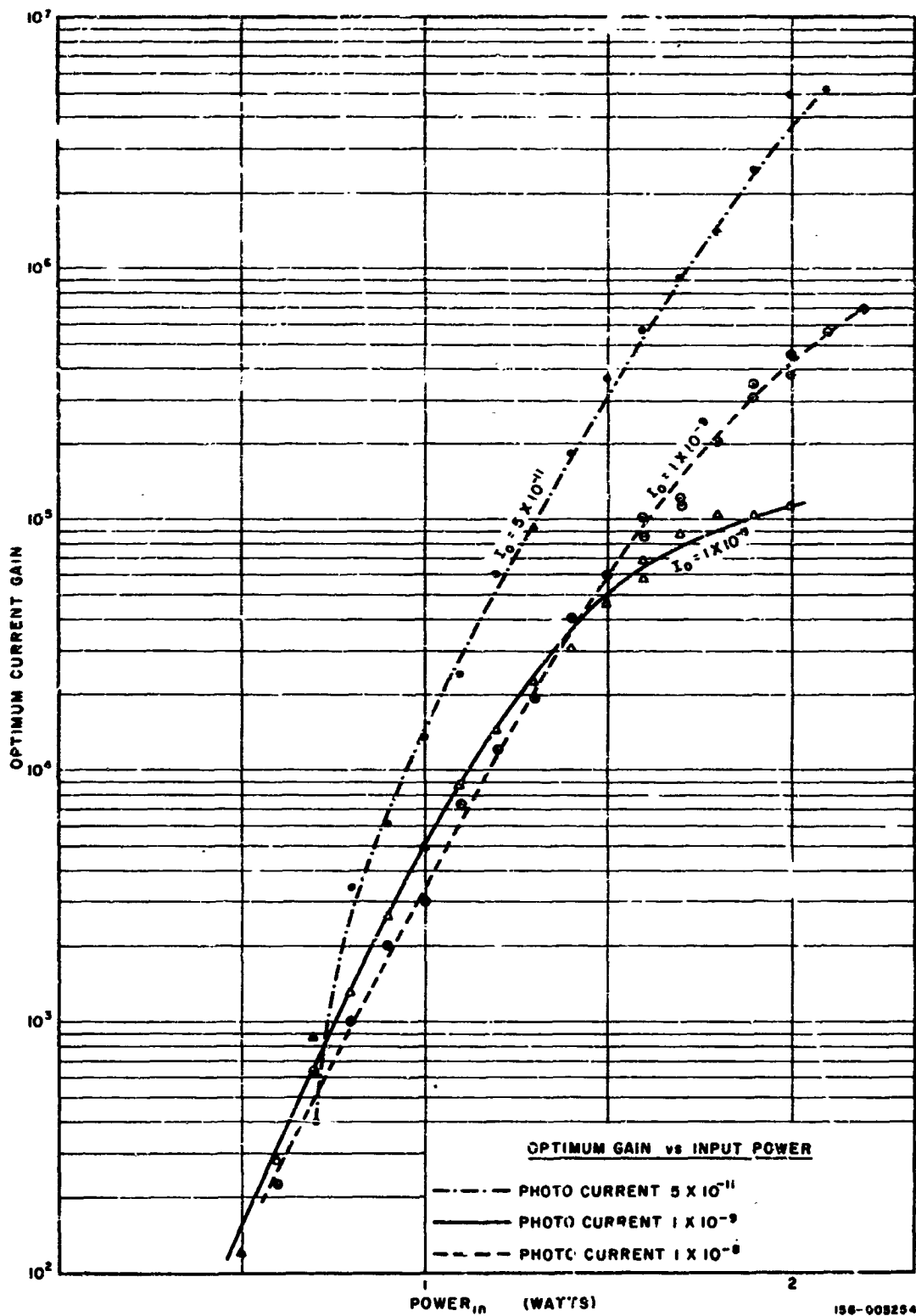


Figure 21. Optimum Current Gain vs Input Power

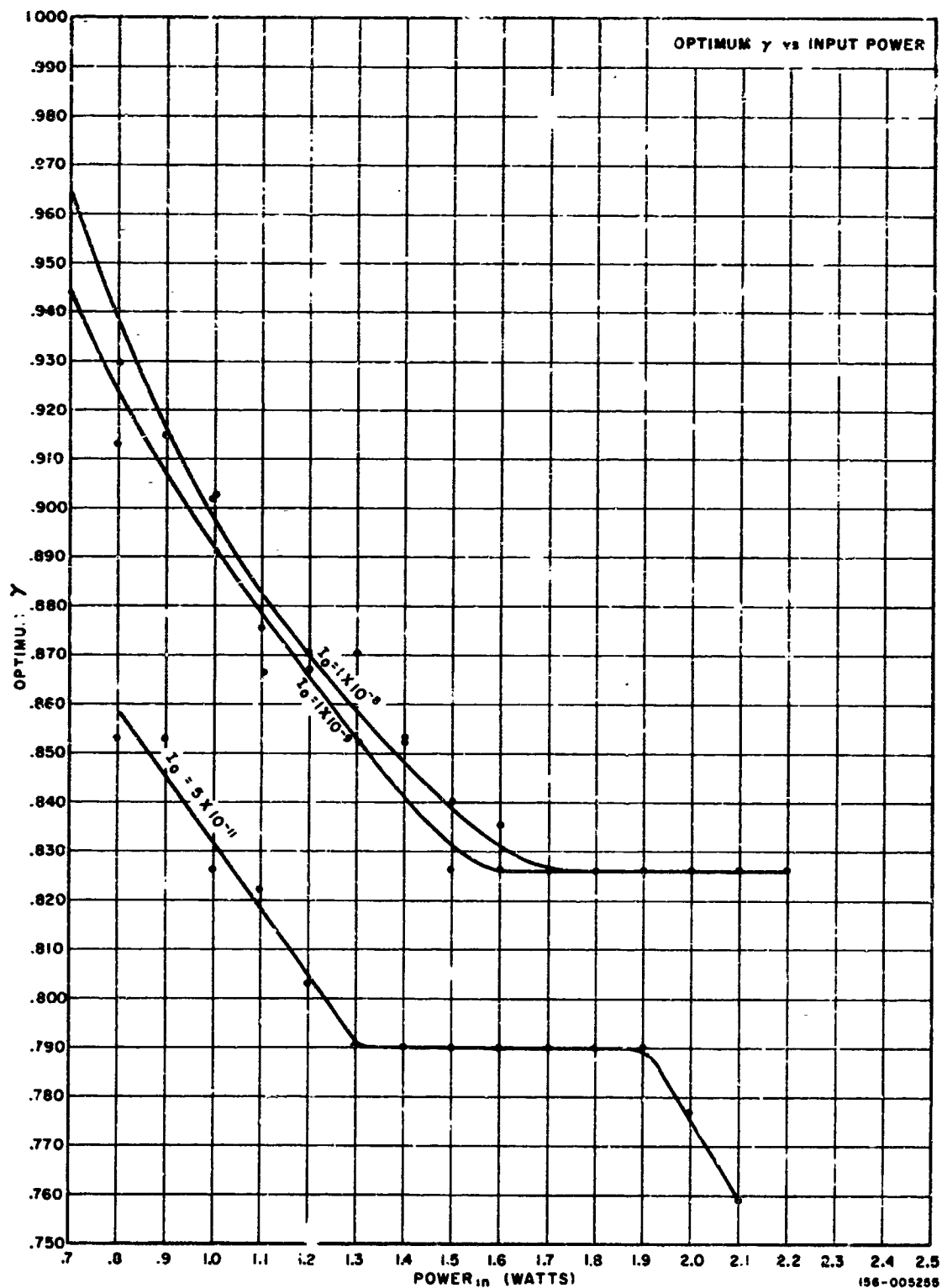


Figure 22. Optimum γ vs Input Power

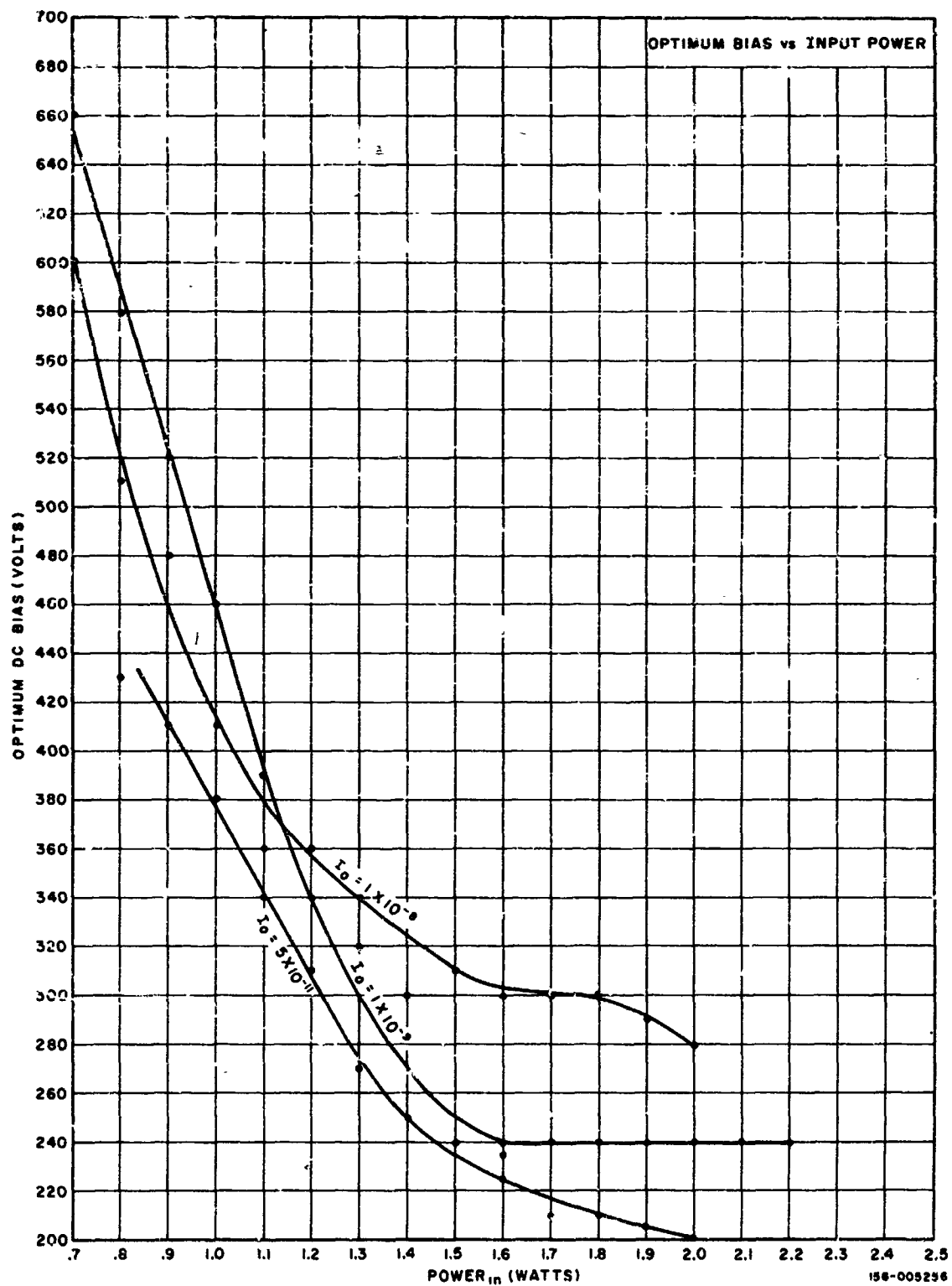


Figure 23. Optimum DC Bias vs Input Power

3.4 Program for Next Reporting Period

The program for the next reporting period will include the construction and evaluation of detectors containing an active electrode (pedestal) of fine molybdenum mesh. The mesh should further reduce, or eliminate instability of the detector. The basic mechanical configuration will be maintained until the advantage of the mesh pedestal has been proven. Another advantage of the mesh is that the pedestal can entirely cover the cathode since the mesh has seventy percent optical transmission.

An investigation of the production of an S-20 Photo-cathode in the DCFEM will be started. This will include possible sub-contractors to produce the surface.

An investigation of the most efficient "getter" will also be included.

3.5 Conclusions and Recommendations

A relatively stable detector has been produced that has high current gain and good frequency response. Its operating life was limited to 100 hours due to internal gassing conditions. This is to be eliminated by further stabilization and proper gettering.

It is recommended that the work continue as outlined in the program for the next reporting period.

BIBLIOGRAPHY

1. A. T. Forrester, et al, Physical Review, 99, 1691 (1955).
2. B. M. Oliver in Proc. of IRE, 48, 1960 (1961) presented the first analysis of laser photomixing with resultant signal-noise ratios. In this connection, see comments by Haus and Townes, Proc. of IRE 49, 1544 (1962) and Oliver same issue, pg. 1545.
3. M. Ross, et al, IRE proc. Nat. Symp. Space Electronics and Telemetry, Oct. 1962.
4. W. S. Read and D. L. Fried, Proc. IEEE, 1787 (1963).